PTEP

Prog. Theor. Exp. Phys. **2026** 013B01 (28 pages)
DOI: 10.1093/ptep/ptaf169

Functional Renormalization Group Flows and Gauge Consistency in Quantum Electrodynamics

Yoshio Echigo [1], Yuji Igarashi [2,†], Katsumi Itoh [2,*], Jan M. Pawlowski [3,‡], and Yu Takahashi [4,§]

[1] *Niigata Polytechnic College, Shibata 957-0017, Japan*
[2] *Faculty of Education, Niigata University, Niigata 950-2181, Japan*
[3] *Institut für Theoretische Physik, Universität Heidelberg, Philosophenweg 16, D-69120 Heidelberg, Germany*
[4] *1196 Sakura-bayashi, Nishikan-ku, Niigata 953-0064, Japan*

Received July 18, 2025; Revised November 3, 2025; Accepted November 4, 2025; Published December 8, 2025

We consider quantum electrodynamics with chiral four-Fermi interactions in the functional renormalization group approach. In gauge theories, the functional flow equation for the effective action is accompanied by the quantum master equation that governs the underlying gauge symmetry. Beyond perturbation theory, fully gauge-consistent solutions are very difficult to obtain. In the present work, by including the lowest-order correction to the photon two-point function, we construct a RG-improved one-loop formula that gives rise to dressed nonperturbative photon propagators in the flow equation as well as the quantum master equation. We show that the one-particle irreducible effective action with the new formula satisfies both equations within our truncations. We also discuss the phase structure in terms of the gauge and four-Fermi couplings based on a numerical solution of the system.

Subject Index B0, B32

1. Introduction

The functional renormalization group (fRG) approach allows for a nonperturbative solution of gauge theories in terms of its renormalization group flow for the gauge-fixed effective action. The underlying gauge symmetry is encoded in modified Ward–Takahashi (mWTI) or Slavnov–Taylor identities (mSTI) that approach the standard ones in the limit of a vanishing (infrared) cutoff scale. A very convenient representation of the symmetry constraints is given by the quantum master equation (QME) [1–4] in the Batalin–Vilkowisky (BV) antifield formalism [5]. For fRG reviews on gauge theories see Refs. [6–12], recent quantum gravity reviews are collected in Ref. [13], a discussion of symmetry constraints in quantum gravity can be found in Ref. [14], a survey of different fRG approaches in gauge theories is provided in Ref. [15], and for further developments see Ref. [16].

The gauge-consistent solution of a gauge theory on a renormalized trajectory (RT) requires approximation schemes for the Wilsonian action S or the corresponding one-particle irreducible (1PI) effective action Γ, whose flow is also a solution of the QME. A further requirement is the necessary *locality* of the construction. This constraint is often neglected; for a

*itoh@ed.niigata-u.ac.jp
†igarashi@ed.niigata-u.ac.jp
‡j.pawlowski@thphys.uni-heidelberg.de
§f15j004a@alumni.niigata-u.ac.jp

Funded by SCOAP^3

discussion of local symmetry operators in the context of chiral symmetry on the lattice see Ref. [17]. It has been shown that within given (finite) truncations there are always nonlocal completions of the flowing effective action that also satisfy the mWTIs or mSTIs; for a detailed discussion see Ref. [7]. In summary, an RT is a *local* truncation of the effective action whose flow satisfies the symmetry identities. While perturbation theory readily offers such a local truncation scheme based on powers of the gauge coupling, the construction of nonperturbative gauge-consistent approximation schemes is obstructed by the requirement of solving two nonlinear functional equations simultaneously.

In the present work we aim at the construction of nonperturbative truncation schemes that lead to RTs within a local implementation of gauge consistency. Within these truncation schemes the flow equations can be solved numerically on RTs. This program is based on a chain of works in the past decade, aiming at perturbative solutions of RTs both in Yang–Mills theory [18] and in quantum electrodynamics (QED) [19]; see also Ref. [20] for the relation between gauge consistency of truncations for the Wilsonian effective action and the 1PI effective action. In these works the algebraic structure of the symmetry identities in the BV formalism played a key role as it linearizes the symmetry constraints in terms of the antifields.

We extend the study in Ref. [19] to nonperturbative resummed flows. Here, we utilize the crucial observation that the perturbative construction in Ref. [19] readily extends to nonperturbative flows. This leads us to an approximately gauge-consistent fRG-flow in QED, including a first numerical solution in a qualitative approximation with four-Fermi terms. Before we set up the construction in detail in the next sections, we want to briefly discuss the underlying structure that allows for this extension: In Ref. [19] we have discussed the one-loop quantum correction of the 1PI effective action, generated by the expansion of the one-loop formula

$$\frac{1}{2}\mathrm{Str}\log\left[\Gamma_{\mathrm{cl}}^{(2)}+\mathcal{R}\right], \tag{1}$$

where the trace Str sums over momenta, Lorentz-, gauge group, and internal indices with a symplectic metric in the fermions. In Eq. (1), $\Gamma_{\mathrm{cl}}^{(2)}$ is the second functional derivative of the classical action Γ_{cl} with respect to the fields, and $\mathcal{R}$ is an infrared regulator term. The one-loop correlation functions derived from the effective action Γ have been shown to be approximate solutions of their flow equations as well as the QMEs or mSTIs. Equation (1) can be readily extended via an RG-improvement to

$$\frac{1}{2}\mathrm{Str}\log\left[(\Gamma_{\mathrm{cl}}+\Gamma_{\mathrm{q}}^{AA})^{(2)}+\mathcal{R}\right], \tag{2}$$

where $\Gamma_{\mathrm{q}}^{AA}$is the lowest-order correction in the photon two-point function. Equation (2) can be understood as the next nonperturbative order in a systematic gauge-consistent skeleton expansion scheme of the flow equation, see Appendix C. The inclusion of such terms accommodates fully dressed photon propagators, while the fermion propagators remain classical. Remarkably, the resulting correlation functions solve approximately both the QME and the flow equations, as we will explain in this paper. Although other important quantum corrections are ignored in this particular truncation, we expect that it will provide a good starting point for further study, partly because our construction is based on the algebraic structure mentioned earlier.

Our ansatz for the 1PI effective action contains the quantum correction for the photon two-point function. The correction term is at $\mathcal{O}(e^2)$ and satisfies both the flow equation and QME. This is consistent with our earlier perturbative result [19].

We numerically studied the flows of the couplings using the 1PI effective action with the above quantum correction, first in the Laudau gauge. We find a unique UV fixed point that determines the RT as well as the phase structure. We have also studied flows including the flow of the gauge parameter ξ and confirmed the uniqueness of the UV fixed point obtained in the Landau gauge. The linear analysis around the UV fixed point including the ξ flow equation gives us an extra relevant direction that is responsible for the $\xi \neq 0$ RT.

QED with four-Fermi couplings has been studied intensively before. These studies aimed at finding a UV fixed point for the theory, and to understand the associated chiral symmetry breaking [21–28]. In particular, the authors of Ref. [28] used the fRG in a different approximation scheme. For a comparison to their result, we calculated the mass anomalous dimension and found a slightly smaller result. Recently, these studies have been extended to QED with a Pauli-term, where a UV fixed point has been found [29,30].

Moreover, gauge-consistent approximations within the flow equation approach have been analyzed extensively, starting with, e.g. Refs. [31,32]. With Eq. (2) we can accommodate the momentum dependence of the flows of correlation functions in a gauge-consistent way. Such momentum-dependent nonperturbative approximations have also been considered in the past three decades. They have found use in particular in QCD, where they are pivotal for quantitative studies of its infrared dynamics. This starts with Refs. [32–34]; for recent quantitative computations see Refs. [35–39] and their review in Ref. [7].

In the next section, a brief summary of the QME and the flow equation is given in the 1PI formulation. We also explain approximations used in this paper. In Section 3 we apply the 1PI effective action to QED with chiral invariant four-Fermi interactions, and show that the correlation functions computed with generic photon propagators solve the QME in our approximation. The correlation functions are confirmed to obey the flow equation; the details are explained in Appendix C. In Section 4 we move on to numerical computations for Λ-evolution of anomalous dimensions, gauge coupling, and four-Fermi couplings. There we use the dimensionless form of the flow equation with the dressed photon propagator for internal lines and anomalous dimensions due to the renormalization. The status of gauge consistency is explained in Section 5. A summary is provided in Section 6.

2. Flow equation and QME for the 1PI effective action

In this section we briefly review the setup within the BV formalism for the flow equation of the 1PI effective action of a generic gauge theory in the fRG, combined with the QME. The latter is obtained via a Legendre transform from its counterparts for the Wilson action, as discussed in Refs. [19,20].

The classical 1PI effective action for a given gauge theory has been shown to be the same as the standard one by an analysis of the BRST-cohomology. Its free part takes the form

$$\Gamma_0[\Phi, \Phi^*] = \frac{1}{2}\Phi^A \left[\frac{1}{\Delta^{(0)}}\right]_{AB} \Phi^B + \Phi^*_A R^A{}_B \Phi^B \,. \tag{3}$$

Here Φ^A denote all species of fields, and their kinetic terms are given by the inverse of the free propagators $\left(\Delta^{(0)}\right)^{AB}$. We use DeWitt's condensed notation: the indices A, B run over spacetime or momenta, internal and Lorentz indices as well as species of fields. The free BRST transformations $R^A{}_B\Phi^B$ for Φ^A are multiplied by their antifields Φ^*_A. By construction, they satisfy the relations

$$\left[\frac{1}{\Delta^{(0)}}\right]_{AC} R^C{}_B + \left[\frac{1}{\Delta^{(0)}}\right]_{BC} R^C{}_A = 0\,. \tag{4}$$

The classical BRST-invariant 1PI effective action also includes the classical interaction $\Gamma_{I,\mathrm{cl}}$,

$$\Gamma_{\mathrm{cl}}[\Phi, \Phi^*] = \Gamma_0[\Phi, \Phi^*] + \Gamma_{I,\mathrm{cl}}[\Phi, \Phi^*]\,. \tag{5}$$

BRST-invariance entails that Eq. (5) solves the classical Master Equation (CME),

$$(\Gamma_{\mathrm{cl}}, \Gamma_{\mathrm{cl}}) = 0\,, \qquad \text{with} \qquad (X, Y) = \frac{\partial^r X}{\partial \Phi^A}\frac{\partial^l Y}{\partial \Phi^*_A} - \frac{\partial^r X}{\partial \Phi^*_A}\frac{\partial^l Y}{\partial \Phi^A}\,, \tag{6}$$

where $\partial^{l(r)}$ denote the left (right) derivative. Once the quantum part Γ_q is included, the 1PI effective action $\Gamma = \Gamma_{\mathrm{cl}} + \Gamma_q$ satisfies the QME,

$$\Sigma = \frac{1}{2}(\Gamma, \Gamma) + \Sigma_K = 0\,. \tag{7}$$

We call the quantity Σ, defined by the second expression of Eq. (7), the quantum master functional. Σ_K is written for $\Gamma_I[\Phi, \Phi^*]$, the interaction part of the 1PI effective action,

$$\Sigma_K = -\mathrm{Tr}\left(K\Gamma^{(2)}_{I*}\frac{1}{1 + \bar{\Delta}^{(0)}\Gamma^{(2)}_I}\right), \tag{8}$$

where $\bar{\Delta}^{(0)}$ is the IR regulated propagator,

$$\bar{\Delta}^{(0)} = (1-K)\Delta^{(0)} = \bar{K}\Delta^{(0)},$$

$$\left(\Gamma^{(2)}_I\right)_{AB} = \frac{\partial^l \partial^r}{\partial \Phi^A \partial \Phi^B}\Gamma_I\,, \qquad \left(\Gamma^{(2)}_{I*}\right)^A{}_B = \frac{\partial^r \partial^l}{\partial \Phi^*_A \partial \Phi^B}\Gamma_I, \tag{9}$$

and the trace Tr sums over includes the multi-indices A, B. In the QME in terms of the Wilsonian action, Σ_K appears as the change of the path integral measure under the BRST transformation. Therefore, we call Σ_K the measure term. $K(u)$ is a function of $u = p^2/\Lambda^2$ where p^2 is the momentum squared and Λ is a cutoff scale. As a regulator function, we require the properties that $K(0) = 1$ and $K(u) \to 0$ sufficiently fast as $u \to \infty$. Due to the function K, Σ_K in Eq. (8) is UV regulated finite. Later we shall observe cancellations of the antibracket term and the measure term in the QME in Eq. (7).

The flow equation for Γ_I is given [40],

$$\dot{\Gamma}_I = \frac{1}{2}\mathrm{Str}\left[\dot{\mathcal{R}}\frac{1}{\Gamma^{(2)} + \mathcal{R}}\right] = -\frac{1}{2}\mathrm{Str}\left(\dot{\bar{\Delta}}^{(0)}\frac{1}{\bar{\Delta}^{(0)}}\frac{1}{1 + \bar{\Delta}^{(0)}\Gamma^{(2)}_I}\right), \tag{10}$$

see also Refs. [41–43]. The dot denotes the derivative with respect to $t = \ln \Lambda/\mu$. Here, μ is a generic reference scale, typically chosen as the initial cutoff scale. The function $\mathcal{R}$ is

$$\mathcal{R}_{AB} = \frac{K}{\bar{K}}\left[\frac{1}{\Delta^{(0)}}\right]_{AB}, \tag{11}$$

with the IR regularization function $\bar{K} = 1 - K$. Now we decompose $\Gamma^{(2)}_I$ as

$$\Gamma^{(2)}_I[\Phi] = \Gamma^{(2)}_I[\Phi = 0] + \tau[\Phi]\,, \tag{12}$$

and define the dressed propagators $\bar{\Delta}$ including quantum corrections as

$$\frac{1}{\bar{\Delta}} = \frac{1}{\bar{\Delta}^{(0)}} + \Gamma^{(2)}_I[\Phi = 0]\,. \tag{13}$$

Note here that $\bar{\Delta}$ is a nonperturbative propagator, which may be expressed as an infinite series of $\Gamma^{(2)}_I[\Phi = 0]$. The field-dependent part $\tau[\Phi]$ gives rise to the interaction vertices. Then, the flow Eq. (10) can be expressed as

$$\dot{\Gamma}_I = -\frac{1}{2}\mathrm{Str}\left[\bar{\Delta}\frac{1}{\bar{\Delta}^{(0)}}\dot{\bar{\Delta}}^{(0)}\frac{1}{\bar{\Delta}^{(0)}}\frac{1}{1+\bar{\Delta}\tau[\Phi]}\right] = \frac{1}{2}\mathrm{Str}\left[\otimes\frac{1}{\bar{\Delta}^{-1}+\tau[\Phi]}\right], \tag{14}$$

where the symbol $\otimes$ represents the regulator,

$$\otimes = \dot{\mathcal{R}} = -\frac{1}{\bar{\Delta}^{(0)}}\dot{\bar{\Delta}}^{(0)}\frac{1}{\bar{\Delta}^{(0)}}\,. \tag{15}$$

We shall use the symbol $\otimes$ in Eq. (15) also in diagrammatic depictions of the flow.

The flow Eq. (10) or (14) has a closed nonperturbative one-loop form, which facilitates the discussion of gauge consistency. We emphasize, however, that the one-loop structure is deceiving in terms of perturbation theory: The full field-dependent propagator incorporates all orders of perturbation theory.

Let us point out that the same full propagator appears in Eq. (8) and gives the one-loop structure for Σ_K.

2.1. *Our approximations*

Solving the two Eqs. (7) and (14) is extremely difficult and approximations are inevitable. In this subsection, we explain approximations used to have our results.

We first observe how the flow Eq. (14) accumulates higher-order quantum corrections. An infinitesimal change of the 1PI effective action is given as,

$$\Gamma_I(t+\Delta t) \sim \Gamma_I(t) + \Delta t \cdot \frac{1}{2}\mathrm{Str}\left[\otimes\frac{1}{\bar{\Delta}^{-1}+\tau[\Phi]}\right](t)\,, \tag{16}$$

where $t = \log \Lambda/\mu$. In the next scale change, $\Gamma_I^{(2)}(t+\Delta t)$ appears on the right-hand side of Eq. (14) as the propagator and the vertices defined in Eqs. (12) and (13).

Let us look at this process more closely by following the flow starting from the classical action Γ_{cl} in Eq. (5) given at some initial scale t_0. In $\Gamma_I(t_0+\Delta t)$ given by Eq. (16), the propagators $\bar{\Delta}$ and vertices $\tau[\Phi]$ are obtained from the classical action Γ_{cl} and the second term on the right-hand side is the perturbative one-loop correction:

$$\Gamma_{\mathrm{cl}} + \Delta t\frac{d}{dt_0}\frac{1}{2}\mathrm{Str}\log\left[\Gamma_{\mathrm{cl}}^{(2)} + \mathcal{R}(t_0)\right]. \tag{17}$$

In the next infinitesimal change of scale, this perturbative one-loop correction contributes to propagators and vertices as described in Eq. (12) and Eq. (13). In this step, $\bar{\Delta}$ acquires nonperturbative contributions. Further scale changes bring nonperturbative corrections to both propagators and vertices.

Integrating the second term of Eq. (17) over $[t,\infty)$, we find the one-loop formula Eq. (1) and the 1PI effective action is given as

$$\Gamma_{\mathrm{cl}} + \Gamma_{\text{one-loop}} \equiv \Gamma_{\mathrm{cl}} + \frac{1}{2}\mathrm{Str}\log\left[\Gamma_{\mathrm{cl}}^{(2)} + \mathcal{R}\right]. \tag{18}$$

In Ref. [19], the QME is studied for the 1PI effective action Eq. (18) for QED: The quantum master functional Σ is written in perturbative approximation as

$$\Sigma = (\Gamma_{\mathrm{cl}}, \Gamma_{\text{one-loop}}) + \Sigma_K|_{\mathrm{cl}}\,. \tag{19}$$

Its AC and $\bar{\Psi}\Psi C$ sectors, denoted as Σ^{AC} and $\Sigma^{\bar{\Psi}\Psi C}$, are found to vanish. Note that we have only the classical action Γ_{cl} in the last term of Eq. (19). For notational simplicity, we drop the symbol $|_{\mathrm{cl}}$ in Eq. (19) from now on. Although we only have proofs for the vanishing of Σ^{AC} and $\Sigma^{\bar{\Psi}\Psi C}$, not the entire functional in Eq. (19), we also know that a Wilsonian action for a generic gauge theory fully satisfies the QME in a one-loop approximation [1] in a different regularization scheme. The vanishing of the entire functional in Eq. (19) remains for a further study.

In this paper, we reconsider Σ^{AC} and $\Sigma^{\bar{\Psi}\Psi C}$ out of Eq. (19) after replacing $\Gamma_{\text{one-loop}}$ with the RG-improved one-loop action Eq. (2): The key element is the RG-improvement for the photon propagator. Surprisingly, we will find in the next section that the two relations $\Sigma^{AC} = 0$ and $\Sigma^{\bar{\Psi}\Psi C} = 0$ hold even after the replacement of photon propagators. In this paper, we only replace the photon propagator; inclusion of quantum corrections to the fermion propagator and vertices and their consistency with the QME are left for future study.

In our numerical study in Section 4, we take an ansatz for the 1PI effective action having the photon two-point function with an unknown function to represent its potential momentum-dependence. The function is determined perturbatively by the flow equation and QME. In the flow of couplings, the photon propagator becomes a nonperturbative one owing to this function. Our numerical results are obtained with these approximations.

3. 1PI effective action and symmetry identities

In the first subsection we construct a 1PI effective action for QED with chiral invariant four-Fermi interactions including quantum corrections described by Eq. (2). The 1PI effective action differs from the one given in Ref. [19] and may be regarded as an extension of it.

In the succeeding subsections, we discuss the QME for the 1PI effective action, then for the vanishing of the quantum master functional Σ in Eq. (7). The important result is that the QME holds for the 1PI effective action with the RG-improved one-loop formula (2) that produces diagrams with the dressed photon propagator. It is worth pointing out that, in our calculations, each term of Σ classified by powers of couplings $e^m G^n$ vanishes by itself and the QME does not produce any relation among the couplings.

In this section, all the couplings are regarded as constant. Later in Section 5 we will reconsider the QME in terms of the renormalized 1PI effective action.

3.1. *1PI effective action*

The free part of the 1PI effective action in QED with a massless Dirac fermion is given by

$$\Gamma_0 = \int_x \left\{ \frac{1}{2} \left[(\partial_\mu A_\nu)^2 - (\partial \cdot A)^2 \right] + \bar{\Psi} i \partial\!\!\!/ \Psi + \left(A^*_\mu - i\partial_\mu \bar{C} \right) \partial_\mu C + \frac{1}{2} \xi B^2 + \left(\bar{C}^* + i\partial \cdot A \right) B \right\} . \tag{20}$$

It contains kinetic terms for the photon A_μ, the massless fermions Ψ and $\bar{\Psi}$, and the Faddeev–Popov ghosts C and $\bar{C}$. In addition to the fields $\Phi^A = \{A_\mu, \Psi, \bar{\Psi}, C, \bar{C}\}$, we also included their antifields $\Phi^*_A = \{A^*_\mu, \Psi^*, \bar{\Psi}^*, C^*, \bar{C}^*\}$. The auxiliary field B and the gauge parameter ξ are introduced for a covariant gauge-fixing. We take the gauge-fixed basis for antifields; for the notation see Ref. [18].

The interaction part of the classical action, $\Gamma_{I,\text{cl}}[\Phi, \Phi^*]$, has two contributions:

$$\Gamma_{I,\text{cl}} = \Gamma_\text{e} + \Gamma_\text{G} . \tag{21}$$

The first term Γ_e consists of the gauge interaction with the gauge coupling e and terms generating BRST transformations on the fermion fields:

$$\Gamma_\text{e} = \int_x \left\{ -e\bar{\Psi} A\!\!\!/ \Psi - ie\Psi^* \Psi C + ie\bar{\Psi}^* \bar{\Psi} C \right\} . \tag{22}$$

We also include chirally invariant four-Fermi interactions:

$$\Gamma_{\mathrm{G}} = \int_x \left\{ \frac{G_S}{2} \left(\left(\bar{\Psi}\Psi\right)\left(\bar{\Psi}\Psi\right) - \left(\bar{\Psi}\gamma_5\Psi\right)\left(\bar{\Psi}\gamma_5\Psi\right) \right) + \frac{G_V}{2} \left(\left(\bar{\Psi}\gamma_\mu\Psi\right)\left(\bar{\Psi}\gamma_\mu\Psi\right) + \left(\bar{\Psi}\gamma_5\gamma_\mu\Psi\right)\left(\bar{\Psi}\gamma_5\gamma_\mu\Psi\right) \right) \right\}. \tag{23}$$

The classical 1PI effective action Γ_{cl},

$$\Gamma_{\mathrm{cl}} = \Gamma_0 + \Gamma_{I,\mathrm{cl}}, \tag{24}$$

is gauge (BRST) invariant or it satisfies the CME (6).

In Ref. [19], we computed the quantum part of the 1PI effective action by expanding the one-loop formula $\mathrm{Str}\log[\Gamma_{\mathrm{cl}}^{(2)} + \mathcal{R}]$. The resulting 1PI effective action is shown to satisfy both the QME and the flow equation.

In this paper, we consider a nonperturbative extension of Ref. [19] by adding a quantum part of the photon two-point function to the classical action Γ_{cl},

$$\Gamma_{\mathrm{q}}^{AA} = \frac{1}{2}\int_{x,y} A_\mu(x)\mathcal{A}_{\mu\nu}(x-y)A_\nu(y)\,, \tag{25}$$

and consider the 1PI effective action Γ with an RG-improved one-loop formula:

$$\begin{aligned} \Gamma &= \Gamma_{\mathrm{cl}} + \Gamma_{\mathrm{q}}, \\ \Gamma_{\mathrm{q}} &= \frac{1}{2}\mathrm{Str}\log[(\Gamma_{\mathrm{cl}} + \Gamma_{\mathrm{q}}^{AA})^{(2)} + \mathcal{R}]. \end{aligned} \tag{26}$$

Equation (26) produces terms constructed with the vertex functions $\tau[\Phi]$ given in Appendix A, the IR-regularized free fermion propagator,

$$\bar{\Delta}^{(0)}_{\alpha\hat{\beta}} = (i\partial\!\!\!/)_{\alpha\hat{\beta}}\bar{\mathbf{\Delta}}^{(0)}\,, \qquad \bar{\mathbf{\Delta}}^{(0)} = \bar{K}/(-\partial^2)\,, \tag{27}$$

and the dressed photon propagator as explained in Eq. (13):

$$\bar{\Delta}_{\mu\nu} = \left(\left(\bar{\Delta}^{(0)}\right)^{-1} + \mathcal{A}\right)^{-1}_{\mu\nu}. \tag{28}$$

In Eq. (28), $\bar{\Delta}^{(0)}_{\mu\nu}$ is the IR-regularized photon free propagator,

$$\bar{\Delta}^{(0)}_{\mu\nu} = (P^T_{\mu\nu} + \xi P^L_{\mu\nu})\bar{\mathbf{\Delta}}^{(0)}\,, \tag{29}$$

where $P^T_{\mu\nu} = \delta_{\mu\nu} - P^L_{\mu\nu},\ P^L_{\mu\nu} = \partial_\mu\partial_\nu/(\partial^2)$ are projection operators. By decomposing $\mathcal{A}_{\mu\nu}$ into the transverse and longitudinal components as

$$\mathcal{A}_{\mu\nu} = \left(\mathcal{T}P^T + \mathcal{L}P^L\right)_{\mu\nu}\,, \tag{30}$$

we obtain the dressed photon propagator,

$$\bar{\Delta}_{\mu\nu} = ((\bar{\Delta}^{(0)})^{-1} + \mathcal{A})^{-1}_{\mu\nu} = \left(P^T T + P^L L\right)_{\mu\nu}\,, \tag{31}$$

where

$$T = \left(-\bar{K}^{-1}\partial^2 + \mathcal{T}\right)^{-1}\,, \qquad L = \left(-\xi^{-1}\bar{K}^{-1}\partial^2 + \mathcal{L}\right)^{-1}\,. \tag{32}$$

Γ_{q} in Eq. (26) produces a series of terms that may be classified by fields attached and the powers of the couplings,

$$\Gamma_{\mathrm{q}} = \Gamma_{\mathrm{q}}^{AA} + \Gamma_{\mathrm{q}}^{\bar{\Psi}\Psi} + \Gamma_{\mathrm{q}}^{\bar{\Psi}A\Psi} + \Gamma_{\mathrm{q}}^{\bar{\Psi}\Psi\bar{\Psi}\Psi} + \cdots\,. \tag{33}$$

Here we only consider terms relevant for later discussions. In Eq. (33), the superscripts indicate the fields attached to terms on the right-hand side. We point out here that terms with internal photon propagators differ from those given in Ref. [19].

Fig. 1. Contributions to $\Gamma_{\mathrm{q}}^{\bar{\Psi}\Psi}$. The thick wavy internal line represents the dressed photon propagator in Eq. (31). The second term vanishes as explained in Ref. [19].

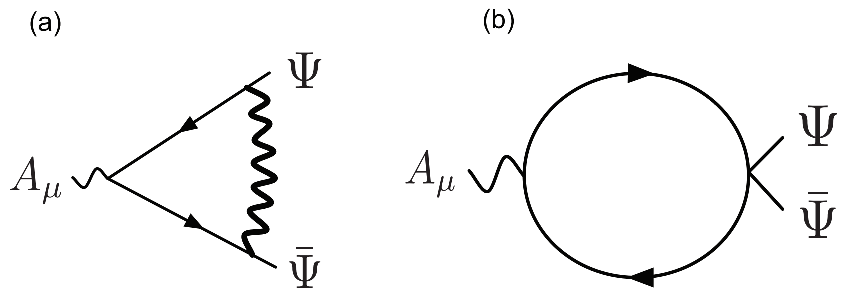

Fig. 2. All the internal propagators are IR regulated. (a) e^3 contribution, $\Gamma_{e^3}^{\bar{\Psi}A\Psi}$. (b) eG contribution, $\Gamma_{e\mathrm{G}}^{\bar{\Psi}A\Psi}$.

The quantum part of the photon two-point function is given as

$$\begin{aligned}\Gamma_{\mathrm{q}}^{AA} = \Gamma_{e^2}^{AA} &= \frac{1}{2}\bar{\Delta}^{(0)}_{\alpha\hat{\alpha}}\tau^{(-\not{A})}_{\hat{\alpha}\beta}\bar{\Delta}^{(0)}_{\beta\hat{\beta}}\tau^{(-\not{A})}_{\hat{\beta}\alpha} \\ &= \frac{1}{2}e^2\int_{x,y}\mathrm{tr}\left((i\not{\partial})\bar{\boldsymbol{\Delta}}^{(0)}(x-y)\not{A}(y)(i\not{\partial})\bar{\boldsymbol{\Delta}}^{(0)}(y-x)\not{A}(x)\right) \\ &\equiv \frac{1}{2}e^2\left[(i\not{\partial})\bar{\boldsymbol{\Delta}}^{(0)}\not{A}(i\not{\partial})\bar{\boldsymbol{\Delta}}^{(0)}\not{A}\right].\end{aligned} \tag{34}$$

The last line of Eq. (34) is the abbreviated expression of the second line: the square bracket on the line implies the trace over spinor indices and the integrations over x and y. The notation $\Gamma_{e^2}^{AA}$ is introduced to show its dependence on the couplings. $\Gamma_{e^2}^{AA}$ in Eq. (34) is generated by a fermion loop and it is the same as that in Ref. [19]. Equation (34) gives $\mathcal{A}_{\mu\nu}$ of Eq. (25).

Now we consider $\Gamma_{\mathrm{q}}^{\bar{\Psi}\Psi}$, $\Gamma_{\mathrm{q}}^{\bar{\Psi}A\Psi}$, and $\Gamma_{\mathrm{q}}^{\bar{\Psi}\Psi\bar{\Psi}\Psi}$ for which the dressed photon propagator (31) may appear in internal lines. The fermion two-point function consists of two terms as depicted in Fig. 1. Though these are the same diagrams as those in Ref. [19], we now use the dressed photon propagator (31) for an internal photon line shown with the thick wavy line in Fig. 1. As explained in Ref. [19], the second diagram vanishes. Therefore, the correction to the fermion two-point function becomes

$$\Gamma_{\mathrm{q}}^{\bar{\Psi}\Psi} = \Gamma_{e^2}^{\bar{\Psi}\Psi} = \bar{\Delta}^{(0)}_{\alpha\hat{\alpha}}\tau^{(-\gamma\Psi)}_{\hat{\alpha}\mu}\bar{\Delta}_{\mu\nu}\tau^{(-\bar{\Psi}\gamma)}_{\nu\alpha} = -e^2\left[\bar{\Delta}_{\mu\nu}\bar{\Psi}\gamma_\nu(i\not{\partial})\bar{\boldsymbol{\Delta}}^{(0)}\gamma_\mu\Psi\right]. \tag{35}$$

The subscript of $\Gamma_{e^2}^{\bar{\Psi}\Psi}$ in Eq. (35) counts the power of couplings attached to vertices. In this paper, we use the same classical vertices as Ref. [19]. Only photon propagators are replaced by Eq. (28). Later the same notation for subscripts is used for the quantum master functionals.

There are two types of quantum corrections to the $\bar{\Psi}\not{A}\Psi$ vertex as shown in Fig. 2:

$$\Gamma_{\mathrm{q}}^{\bar{\Psi}A\Psi} = \Gamma_{e^3}^{\bar{\Psi}A\Psi} + \Gamma_{e\mathrm{G}}^{\bar{\Psi}A\Psi}. \tag{36}$$

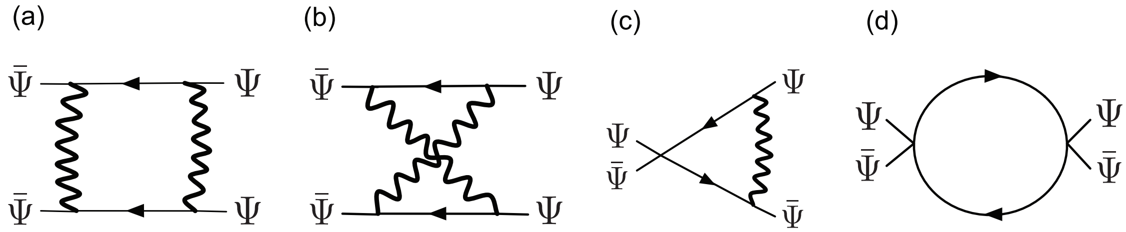

Fig. 3. (a) $\Gamma^{\bar{\Psi}\Psi\bar{\Psi}\Psi}_{e^4}$. (b) $\Gamma^{\bar{\Psi}\Psi\bar{\Psi}\Psi}_{e^4}$, non-planar contributions. (c) $\Gamma^{\bar{\Psi}\Psi\bar{\Psi}\Psi}_{e^2\mathrm{G}}$. (d) $\Gamma^{\bar{\Psi}\Psi\bar{\Psi}\Psi}_{\mathrm{G}^2}$. RG-one-loop diagrams for $\Gamma^{\bar{\Psi}\Psi\bar{\Psi}\Psi}_{\mathrm{q}}$. There are variations in connecting fermion lines to four-Fermi vertices other than (c) and (d).

The first term $\Gamma^{\bar{\Psi}A\Psi}_{e^3}$ is generated solely with the gauge interaction and

$$\begin{aligned}\Gamma^{\bar{\Psi}A\Psi}_{e^3} &= \frac{1}{3}\Big[-\bar{\Delta}^{(0)}_{\alpha\hat{\alpha}}\Big(\tau^{(-\gamma\Psi)}_{\hat{\alpha}\mu}\bar{\Delta}_{\mu\nu}\tau^{(-\bar{\Psi}\gamma)}_{\nu\beta}\bar{\Delta}^{(0)}_{\beta\hat{\beta}}\tau^{(-\not{A})}_{\hat{\beta}\alpha} - \tau^{(-\not{A})}_{\hat{\alpha}\beta}\bar{\Delta}^{(0)}_{\beta\hat{\beta}}\tau^{(-\gamma\Psi)}_{\hat{\beta}\mu}\bar{\Delta}_{\mu\nu}\tau^{(-\bar{\Psi}\gamma)}_{\nu\alpha}\Big) \\ &\qquad + \bar{\Delta}_{\mu\nu}\tau^{(-\bar{\Psi}\gamma)}_{\nu\alpha}\bar{\Delta}^{(0)}_{\alpha\hat{\alpha}}\tau^{(-\not{A})}_{\hat{\alpha}\beta}\bar{\Delta}^{(0)}_{\beta\hat{\beta}}\tau^{(-\gamma\Psi)}_{\hat{\beta}\mu}\Big] \\ &= -e^3\Big[\bar{\Delta}_{\mu\nu}\bar{\Psi}\gamma_\nu(i\not{\partial})\bar{\boldsymbol{\Delta}}^{(0)}\not{A}(i\not{\partial})\bar{\boldsymbol{\Delta}}^{(0)}\gamma_\mu\Psi\Big]. \end{aligned} \tag{37}$$

The second term $\Gamma^{\bar{\Psi}A\Psi}_{e\mathrm{G}}$ in Eq. (36) with four-Fermi interactions is given by

$$\begin{aligned}\Gamma^{\bar{\Psi}A\Psi}_{e\mathrm{G}} &= \bar{\Delta}^{(0)}_{\alpha\hat{\alpha}}\tau^{(-\not{A})}_{\hat{\alpha}\beta}\bar{\Delta}^{(0)}_{\beta\hat{\beta}}\tau^{\bar{\Psi}\Psi}_{\hat{\beta}\alpha} \\ &= 2e\,G_S\Big[\bar{\Psi}(i\not{\partial})\bar{\boldsymbol{\Delta}}^{(0)}\not{A}(i\not{\partial})\bar{\boldsymbol{\Delta}}^{(0)}\Psi\Big] + 2eG_V\Big[\bar{\Psi}\gamma_\mu(i\not{\partial})\bar{\boldsymbol{\Delta}}^{(0)}\not{A}(i\not{\partial})\bar{\boldsymbol{\Delta}}^{(0)}\gamma_\mu\Psi\Big] \\ &\quad -4eG_V\Big[i\partial_\rho\bar{\boldsymbol{\Delta}}^{(0)}A_\rho i\partial_\mu\bar{\boldsymbol{\Delta}}^{(0)} - i\partial_\rho\bar{\boldsymbol{\Delta}}^{(0)}A_\mu i\partial_\rho\bar{\boldsymbol{\Delta}}^{(0)} + i\partial_\mu\bar{\boldsymbol{\Delta}}^{(0)}A_\rho i\partial_\rho\bar{\boldsymbol{\Delta}}^{(0)}\Big]\big(\bar{\Psi}\gamma_\mu\Psi\big). \end{aligned} \tag{38}$$

We emphasize that $\Gamma^{\bar{\Psi}\Psi}_{e^2}$ and $\Gamma^{\bar{\Psi}A\Psi}_{e^3}$ have the dressed photon propagators (28) whereas the loops for $\Gamma^{AA}_{e^2}$ and $\Gamma^{\bar{\Psi}A\Psi}_{e\mathrm{G}}$ contain only the IR-regulated free fermion propagators (27) and, therefore, are the same as those given in Ref. [19].

The quantum corrections to four-Fermi interactions consist of the contributions proportional to e^4, e^2G, and G^2: $\Gamma^{\bar{\Psi}\Psi\bar{\Psi}\Psi}_{\mathrm{q}} = \Gamma^{\bar{\Psi}\Psi\bar{\Psi}\Psi}_{e^4} + \Gamma^{\bar{\Psi}\Psi\bar{\Psi}\Psi}_{e^2\mathrm{G}} + \Gamma^{\bar{\Psi}\Psi\bar{\Psi}\Psi}_{\mathrm{G}^2}$. Since they are not necessary in our discussions for the QME, we only show diagrams in Fig. 3. These diagrams will be helpful to understand the discussions in Section 4.4. There are variations in connecting fermion lines to four-Fermi vertices other than Fig. 3(c) and 3(d).

3.2. *QME for the AC-sector*

The quantum master functional Σ in Eq. (7) can be decomposed into a sum of products of fields. In QED, each product consists of the ghost C multiplied by a monomial of the photon fields A_μ and/or the fermion fields Ψ and $\bar{\Psi}$. Here we consider two types of products, AC and $\bar{\Psi}\Psi C$, denoted as Σ^{AC} and $\Sigma^{\bar{\Psi}\Psi C}$.

Let us first consider Σ^{AC}. It is given by

$$\Sigma^{AC} = \Sigma^{AC}_{e^2} = (\Gamma_0,\ \Gamma^{AA}_{\mathrm{q}}) + \Sigma^{AC}_K. \tag{39}$$

The bracketed term in Eq. (39) is the BRST transformation of Γ^{AA}_{q} in Eq. (34), which is a fermion one-loop proportional to e^2. The measure term Σ_K in Eq. (8) contains a vertex $\Gamma^{(2)}_{I*} \propto eC$. The AC term of Σ_K is obtained by taking another vertex $\tau^{(-\not{A})} \propto e\not{A}$ (or $\tau^{(\not{A}^T)}$) attached to a fermion loop. Therefore, Σ^{AC}_K is also proportional to e^2. The expressions of the vertices are listed in Appendix A. Since all propagators in Eq. (39) are fermionic, $\Sigma^{AC}_{e^2}$ is the same as the one computed in Ref. [19] that was shown to vanish: $\Sigma^{AC}_{e^2} = 0$.

The condition $\Sigma^{AC}_{e^2} = 0$ determines the longitudinal component $\mathcal{L}$ in Eq. (30) from its measure term Σ^{AC}_K. $\mathcal{L}$ calculated from the one-loop formula (26) gives the same function as the one from $\Sigma^{AC}_{e^2} = 0$. For later use, we give the expression for $\mathcal{L}$ given in Refs. [20] and [19]:

$$\mathcal{L}(p) = -8e^2 \int_q K(p+q)\bar{K}(q)\frac{(p\cdot q)}{p^2q^2}\,, \qquad \int_q = \int \frac{d^4q}{(2\pi)^4}\,. \tag{40}$$

Having the regulator functions K and $\bar{K}$, the integral in Eq. (40) gives a finite result. In the limit $\Lambda \to 0$, the function $\mathcal{L}$ vanishes as expected.

3.3. *QME for the $\bar{\Psi}\Psi C$ sector*

The quantum master functional for the $\bar{\Psi}\Psi C$ sector consists of two parts distinguished by powers of couplings:

$$\Sigma^{\bar{\Psi}\Psi C} = \Sigma^{\bar{\Psi}\Psi C}_{e^3} + \Sigma^{\bar{\Psi}\Psi C}_{e\mathrm{G}}\,. \tag{41}$$

It follows from Eq. (7) that

$$\begin{aligned}\Sigma^{\bar{\Psi}\Psi C}_{e^3} &= (\Gamma_e, \Gamma^{\bar{\Psi}\Psi}_{e^2}) + (\Gamma_0, \Gamma^{\bar{\Psi}A\Psi}_{e^3}) + \Sigma^{\bar{\Psi}\Psi C}_{K\ e^3},\\ \Sigma^{\bar{\Psi}\Psi C}_{e\mathrm{G}} &= (\Gamma_0, \Gamma^{\bar{\Psi}A\Psi}_{e\mathrm{G}}) + \Sigma^{\bar{\Psi}\Psi C}_{K\ e\mathrm{G}}.\end{aligned} \tag{42}$$

$\Sigma^{\bar{\Psi}\Psi C}_{e\mathrm{G}}$ in Eqs. (42) involves only fermion loops and we already showed its vanishing in Ref. [19]. The subscripts of Σ in Eq. (41) and Eqs. (42) count powers of couplings attached to vertices.

The antibracket contributions in the first equation in Eqs. (42) are given as

$$\begin{aligned}(\Gamma_e, \Gamma^{\bar{\Psi}\Psi}_{e^2}) &= e^3\left[\bar{\Psi}\gamma_\nu \not{\partial}\bar{\mathbf{\Delta}}^{(0)} C\gamma_\mu\Psi\bar{\Delta}_{\mu\nu}\right] - e^3\left[\bar{\Psi}\gamma_\nu C\not{\partial}\bar{\mathbf{\Delta}}^{(0)}\gamma_\mu\Psi\bar{\Delta}_{\mu\nu}\right],\\ (\Gamma_0, \Gamma^{\bar{\Psi}A\Psi}_{e^3}) &= -e^3\left[\bar{\Psi}\gamma_\nu\not{\partial}\bar{\mathbf{\Delta}}^{(0)}\not{\partial}C\not{\partial}\bar{\mathbf{\Delta}}^{(0)}\gamma_\mu\Psi\bar{\Delta}_{\mu\nu}\right]\\ &= e^3\left[\bar{\Psi}\gamma_\nu(1-K)C\not{\partial}\bar{\mathbf{\Delta}}^{(0)}\gamma_\mu\Psi\bar{\Delta}_{\mu\nu}\right] - e^3\left[\bar{\Psi}\gamma_\nu\not{\partial}\bar{\mathbf{\Delta}}^{(0)}C(1-K)\gamma_\mu\Psi\bar{\Delta}_{\mu\nu}\right],\end{aligned} \tag{43}$$

by using integration by parts and $\partial^2\bar{\mathbf{\Delta}}^{(0)} = -\bar{K}$. The measure part reads

$$\begin{aligned}\Sigma^{\bar{\Psi}\Psi C}_{K\ e^3} &= -\left[K\tau^C_{*\alpha\beta}\bar{\Delta}^{(0)}_{\beta\hat{\alpha}}\tau^{(-\gamma\Psi)}_{\hat{\alpha}\mu}\bar{\Delta}_{\mu\nu}\tau^{(-\bar{\Psi}\gamma)}_{\nu\alpha} + K\tau^C_{*\hat{\alpha}\hat{\beta}}\bar{\Delta}^{(0)}_{\hat{\beta}\alpha}\tau^{(\bar{\Psi}\gamma)}_{\alpha\mu}\bar{\Delta}_{\mu\nu}\tau^{(\gamma\Psi)}_{\nu\hat{\alpha}}\right]\\ &= e^3\left[\bar{\Psi}\gamma_\nu KC\not{\partial}\bar{\mathbf{\Delta}}^{(0)}\gamma_\mu\Psi\bar{\Delta}_{\mu\nu}\right] - e^3\left[\bar{\Psi}\gamma_\mu\not{\partial}\bar{\mathbf{\Delta}}^{(0)}CK\gamma_\nu\Psi\bar{\Delta}_{\mu\nu}\right].\end{aligned} \tag{44}$$

By summing up Eqs. (43) and (44), we confirm that

$$\Sigma^{\bar{\Psi}\Psi C}_{e^3} = (\Gamma_e, \Gamma^{\bar{\Psi}\Psi}_{e^2}) + (\Gamma_0, \Gamma^{\bar{\Psi}A\Psi}_{e^3}) + \Sigma^{\bar{\Psi}\Psi C}_{K\ e^3} = 0\,. \tag{45}$$

Therefore, $\Sigma^{\bar{\Psi}\Psi C} = \Sigma^{\bar{\Psi}\Psi C}_{e^3} + \Sigma^{\bar{\Psi}\Psi C}_{e\mathrm{G}} = 0$.

In conclusion, we have shown $\Sigma^{AC} = \Sigma^{\bar{\Psi}\Psi C} = 0$. Let us point out here that the photon propagator $\bar{\Delta}_{\mu\nu}$ behaves as a spectator in the proof of $\Sigma^{\bar{\Psi}\Psi C} = 0$: a particular form of the photon propagator $\bar{\Delta}_{\mu\nu}$ is not required to show the condition.

Note that the QME for the 1PI effective action (26) does not produce any relations among the couplings. The authors of Refs. [44] and [45] obtained a constraint between the gauge and four-Fermi couplings out of the mWTI and discussed its physical implications. In our earlier publication [20], we also had a relation among couplings when we keep generic form factors for various vertices. This implies that constraints among couplings out of the QME depend on an ansatz for the 1PI effective action. We may understand that the 1PI effective actions in the present work and our perturbative studies [18,19] have particular form factors so that each of the terms, classified by the powers $e^n G^m_{S,V}$, vanishes by itself. This is an intriguing possibility and a comprehensive discussion will be provided elsewhere.

4. Numerical study

Here we introduce our ansatz including the quantum correction for the photon two-point function, which give rise to the momentum-dependent form factor. This is preceded by a derivation of the dimensionless form of the flow equation. The numerical results are explained and compared with earlier studies.

4.1. *Z factors and inclusion of anomalous dimensions*

Let us introduce anomalous dimensions into the flow equations, rescaling the fields as $\Phi^A = Z_A^{1/2}\Phi^A_{(r)}$ with the wave function renormalization Z_A. The regulator terms (11) are replaced by $Z_A\mathcal{R}_{AB}$ on which the $\Lambda\partial_\Lambda = \partial_t$ derivative on the right-hand side of the flow equations in Eq. (10) acts as

$$\partial_t\left(Z_A\mathcal{R}_{AB}\right) = Z_A\left[\dot{\mathcal{R}}_{AB} - \eta_A\mathcal{R}_{AB}\right], \tag{46}$$

where

$$\eta_A = -\partial_t \ln Z_A \tag{47}$$

denotes anomalous dimensions for Φ^A. For our correlation functions, Γ^{AA}_{q}, $\Gamma^{\bar\Psi\Psi}_{\mathrm{q}}$, $\Gamma^{\bar\Psi A\Psi}_{\mathrm{q}}$, and $\Gamma^{\bar\Psi\Psi\bar\Psi\Psi}_{\mathrm{q}}$, ∂_t acts on the free propagators. Since

$$\begin{aligned}\dot{\mathcal{R}} - \eta\mathcal{R} &= (\partial_t - \eta)\frac{K}{\bar K}\left(\Delta^{(0)}\right)^{-1} = \partial_t\left(\bar\Delta^{(0)}\right)^{-1} - \eta K\left(\bar\Delta^{(0)}\right)^{-1}\\ &= -\left(\bar\Delta^{(0)}\right)^{-1}\left[\left(\partial_t + \eta K\right)\bar\Delta^{(0)}\right]\left(\bar\Delta^{(0)}\right)^{-1},\end{aligned} \tag{48}$$

the anomalous dimensions can be included by the replacement $\partial_t\bar\Delta^{(0)} \to \left(\partial_t + \eta K\right)\bar\Delta^{(0)}$. Note that the factor K multiplied by η makes the flow equations UV finite. Using this prescription, we show that our correlation functions fulfill the flow equations with anomalous dimensions. In our case, the corresponding Z factors are defined as

$$\begin{aligned}&A_{(r)\mu} = Z_3^{1/2}A_\mu,\ A^*_{(r)\mu} = Z_3^{-1/2}A^*_\mu,\ B_{(r)} = Z_3^{-1/2}B,\\ &C_{(r)} = Z_3^{1/2}C,\quad \bar C_{(r)} = Z_3^{-1/2}\bar C,\quad \bar C^*_{(r)} = Z_3^{1/2}\bar C^*,\\ &\Psi_{(r)} = Z_2^{1/2}\Psi,\quad \Psi^*_{(r)} = Z_2^{-1/2}\Psi^*,\ \ \bar\Psi_{(r)} = Z_2^{1/2}\bar\Psi,\ \bar\Psi^*_{(r)} = Z_2^{-1/2}\Psi^*.\end{aligned}$$

Note that the transformations $\Phi^A_{(r)} = Z_A^{1/2}\Phi^A$ and $\Phi^*_{(r)A} = Z_A^{-1/2}\Phi^*_A$ in Eqs. (49) are canonical transformations in the space of fields and antifields. For the couplings and the gauge parameter, we set

$$e_{(r)} = e(t) = Z_e e,\qquad G_{(r)S,V} = G_{S,V}(t) = Z_{S,V}\cdot\Lambda^2 G_{S,V},\qquad \xi_{(r)} = \xi(t) = Z_3\xi\,. \tag{50}$$

Here we introduced the notation $e(t)$, $G_{S,V}(t)$, and $\xi(t)$ for the corresponding renormalized quantities for later convenience. After making all the quantities dimensionless, we find the flow equation in 4D momentum space as

$$\begin{aligned}\partial_t\Gamma[\hat\Phi_{(r)}]\,|_{\hat\Phi_{(r)}} &= \frac{1}{2}(-)^{\epsilon_A}\int_{\hat p}\left[\partial_t\hat{\mathcal{R}} - \eta\,\hat{\mathcal{R}}\right]_{AB}\left[\left(\frac{\partial^l\partial^r\Gamma}{\partial\hat\Phi_{(r)}\partial\hat\Phi_{(r)}} + \hat{\mathcal{R}}\right)^{-1}\right]^{BA}(\hat p,\hat p) - 4\,\Gamma[\hat\Phi_{(r)}]\\ &\quad + \left(d_A + \eta_A/2\right)\int_{\hat p}\hat\Phi^A_{(r)}(\hat p)\frac{\partial^l\Gamma[\hat\Phi_{(r)}]}{\partial\hat\Phi^A_{(r)}(\hat p)} + \int_{\hat p}\hat\Phi^A_{(r)}(\hat p)\,\hat p\cdot\frac{\partial'}{\partial\hat p}\left(\frac{\partial^l\Gamma[\hat\Phi_{(r)}]}{\partial\hat\Phi^A_{(r)}(\hat p)}\right),\end{aligned} \tag{51}$$

where $\hat{p} = p/\Lambda$, $\hat{\mathcal{R}}_{AB} = \Lambda^{d_A+d_B-d}\mathcal{R}_{AB}$, and $\hat{\Phi}^A_{(r)}(\hat{p}) = \Lambda^{d-d_A}\Phi^A_{(r)}(p)$ for the renormalized fields $\Phi^A_{(r)}(p)$ with canonical dimensions d_A. The t-derivative on the left-hand side is now taken for fixed $\hat{\Phi}^A_{(r)}$. The prime of $\partial'/\partial\hat{p}$ on the right-hand side implies that the derivative does not act on the delta function for momentum conservation. $\partial_t\hat{\mathcal{R}} - \eta\,\hat{\mathcal{R}}$ is the dimensionless form of the quantity defined in Eq. (15) and the same symbol $\otimes$ will be used to represent it.

We used the hatted notations to denote dimensionless quantities in Eq. (51). From now on we drop the hats for simplicity. In our 1PI effective action in Section 3, the antifield appears only to define the BRST transformations and no 1PI diagrams are present to change the terms. The scale changes of the terms with antifields are due to the Z factors described above and we can easily recover those scale changes if necessary. Based on these observations, we ignore the terms with antifields in this section.

Note that the quantum corrections collected by using Eq. (51) differ from Eq. (2). See Appendix C.2 and Appendix C.3 for details.

4.2. *Ansatz for the dimensionless 1PI effective action*

From Eq. (20) we eliminate all antifields $\Phi^*_A = 0$ and the B field to obtain the free action

$$\Gamma_0 = \int_p \left[\frac{1}{2}A_\mu(-p)\left[\delta_{\mu\nu}p^2 + (\xi(t)^{-1} - 1)p_\mu p_\nu\right]A_\nu(p) + \bar{\Psi}(-p)\not{p}\Psi(-p)\right]. \tag{52}$$

The classical interaction part is given by

$$\begin{aligned}\Gamma_{I,\mathrm{cl}} = -e(t)\int_{p,q}\bar{\Psi}(-p)\not{A}(p-q)\Psi(q) + \frac{1}{2}\int_{p_1,\cdots,p_4}(2\pi)^4\delta^4(p_1+p_2+p_3+p_4)\\ \times\left[G_S(t)\left\{\left(\bar{\Psi}(p_1)\Psi(p_2)\right)\left(\bar{\Psi}(p_3)\Psi(p_4)\right) - \left(\bar{\Psi}(p_1)\gamma_5\Psi(p_2)\right)\left(\bar{\Psi}(p_3)\gamma_5\Psi(p_4)\right)\right\}\right.\\ \left. + G_V(t)\left\{\left(\bar{\Psi}(p_1)\gamma_\mu\Psi(p_2)\right)\left(\bar{\Psi}(p_3)\gamma_\mu\Psi(p_4)\right) + \left(\bar{\Psi}(p_1)\gamma_5\gamma_\mu\Psi(p_2)\right)\left(\bar{\Psi}(p_3)\gamma_5\gamma_\mu\Psi(p_4)\right)\right\}\right]\end{aligned} \tag{53}$$

If we take the classical 1PI effective action $\Gamma_{\mathrm{cl}} = \Gamma_0 + \Gamma_{I,\mathrm{cl}}$, $[\Gamma^{(2)}_{\mathrm{cl}} + \mathcal{R}]^{-1}$ in Eq. (51) can be expanded in terms of the IR-regularized free propagators, $\bar{\Delta}^{(0)}_{\alpha\hat{\beta}}$ and $\bar{\Delta}^{(0)}_{\mu\nu}$, and the vertices generated from $\Gamma_{I,\mathrm{cl}}$. It leads to a truncation of the flow equations at the lowest order in couplings.

As discussed in Section 3, we proceed beyond the lowest-order computation by including the quantum correction to the photon two-point function:

$$\begin{aligned}\Gamma^{AA}_{e^2} &= \tfrac{1}{2}\int_p A_\mu(-p)\mathcal{A}_{\mu\nu}(t,p)A_\nu(p)\,,\\ \mathcal{A}_{\mu\nu}(t,p) &= P^T_{\mu\nu}\mathcal{T}(t,p^2) + P^L_{\mu\nu}\mathcal{L}(t,p^2)\,.\end{aligned} \tag{54}$$

The two functions $\mathcal{T}(t,p^2)$ and $\mathcal{L}(t,p^2)$ are computed from their flows.

Finally, our ansatz for the 1PI effective action is given by

$$\Gamma = \Gamma_{\mathrm{cl}} + \Gamma^{AA}_{e^2}\,. \tag{55}$$

With the inclusion of $\mathcal{A}_{\mu\nu}$ the IR-regularized free propagators $\bar{\Delta}^{(0)}_{\mu\nu}$ are replaced by the dressed one, $\bar{\Delta}_{\mu\nu} = \left(\left(\bar{\Delta}^{(0)}\right)^{-1} + \mathcal{A}\right)^{-1}_{\mu\nu}$.

With the ansatz (55), the right-hand side of the flow Eq. (51) is constructed with the dressed photon propagator, the free fermion propagator, and the classical interaction vertices that give rise to the same quantum corrections discussed in Section 3 with appropriately inserted regulator terms. Though we do not have momentum-dependent form factors for the fermion two-point function and interaction vertices, this does not imply that we ignore all the quantum corrections to them. In writing down the flow equations for the couplings, we extract the con-

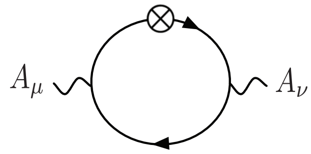

Fig. 4. One-loop diagram which contributes to the photon two-point function. The symbol $\otimes$ represents the regulator $\partial_t \mathcal{R} - \eta \mathcal{R}$ in the flow Eq. (51).

stant parts from the form factors for the fermion two-point function and the interaction terms to find the flow equations for the couplings. In this process, we extract the Z factors out of the quantum corrections.

Inclusion of $\Gamma^{AA}_{e^2}$ in the ansatz (55) allows us to find the momentum-dependent quantum correction that is consistent with the flow equation and the QME in the lowest order in the coupling e^2.

4.3. *Quantum corrections to photon two-point function*

We compute $\mathcal{A}_{\mu\nu}$ in Eq. (54) by solving the dimensionless flow equations (51) with a specific cutoff function $K(x) = \exp(-x)$ where $x = p^2$. In this subsection we describe only the results and leave further details in Appendix B.

From the functional flow Eq. (51), we collect terms with two photon fields $A_\mu A_\nu$ and obtain the flow equation for $\mathcal{A}_{\mu\nu}$. Figure 4 shows the one-loop contribution on the right-hand side of Eq. (51). The x-linear terms in the flow equation for $\mathcal{A}_{\mu\nu}$ have particular roles: They give rise to an algebraic relation (B4) for the anomalous dimensions and the flow equation for the gauge parameter to be presented shortly. Similarly, from the flow equation for the fermion two-point function, we find that $\not{p}$-linear terms give rise to another relation (B19) of anomalous dimensions.

The flow equation for $\mathcal{A}_{\mu\nu}$ leads to the differential equations for $\mathcal{T}$ and $\mathcal{L}$: At the lowest order in the coupling $\alpha(t) = e^2(t)$, they are

$$
\begin{aligned}
\left(x\frac{\partial}{\partial x} - 1\right)\mathcal{T}(t,x) &= -\frac{\alpha}{8\pi^2 x^2}\left\{4 + \frac{2x^3}{3} - \left(4 + 2x - x^2\right)\exp(-x/2)\right\},\\
\left(x\frac{\partial}{\partial x} - 1\right)\mathcal{L}(t,x) &= \frac{\alpha}{8\pi^2 x^2}\left\{12 - 8x - \left(12 - 2x - x^2\right)\exp(-x/2)\right\}.
\end{aligned}
\tag{56}
$$

Solving Eq. (56), we obtain

$$
\begin{aligned}
\mathcal{T}(t,x) &= \frac{\alpha(t)}{6\pi^2 x^2}\left[1 - \left(1 + \frac{x}{2} - x^2\right)\exp(-x/2) + \frac{x^3}{2}\left(\mathrm{Ei}(-x/2) - \log x\right)\right] + c_T x,\\
\mathcal{L}(t,x) &= -\frac{\alpha(t)}{2\pi^2 x^2}\left[1 - x - \left(1 - \frac{x}{2}\right)\exp(-x/2)\right] + c_L x,
\end{aligned}
\tag{57}
$$

where Ei is the exponential integral defined as,

$$
\mathrm{Ei}(-x/2) = \int_\infty^{x/2} \frac{e^{-u}}{u} du\,. \tag{58}
$$

Note that $\mathcal{T}$ and $\mathcal{L}$ are t-dependent quantities through their dependence on $\alpha(t)$. Here, c_T and c_L are integration constants. Here it is worth pointing out that the potentially divergent contributions in the diagram to define $\mathcal{A}_{\mu\nu}$ are contained in the integration constants. Presently we find that those constants should take finite values and, therefore, both $\mathcal{T}$ and $\mathcal{L}$ are finite functions.

The condition $\Sigma^{AC} = 0$ determines the longitudinal part $\mathcal{L}$ in the photon two-point functions $\mathcal{A}_{\mu\nu}$. In momentum space, it is given as

$$\mathcal{L}(t, x = p^2) = -8\alpha(t) \int_q K(p+q)\bar{K}(q) \frac{(p \cdot q)}{p^2 q^2}, \tag{59}$$

which is Eq. (40) in its dimensionless form. For our choice $K(x) = \exp(-x)$, Eq. (59) gives $\mathcal{L}(t, x)$ in Eq. (57) with $c_L = 0$ [20]: The consistency with the QME requires $c_L = 0$. Since we have already renormalized fields, the x-linear term should be absent in $\mathcal{T}$. This condition gives us

$$c_T = \frac{1}{12\pi^2}\left(\frac{13}{12} - \gamma + \log 2\right), \tag{60}$$

where γ is Euler's constant.

As we mentioned earlier, the flow equation for the photon two-point function, obtained from Eq. (51), contains x-linear terms in both the transverse and longitudinal parts. Those in the longitudinal part give the flow equation for the gauge parameter:

$$\partial_t \xi = -\xi \cdot \eta_A(\alpha, \xi). \tag{61}$$

Appendix B contains its derivation. From Eq. (61) it is obvious that the Landau gauge stays in the gauge along an RG flow.

Two algebraic relations [Eqs. (B4) and (B19)] are solved to give η_A and η_ψ as

$$\begin{aligned}
\eta_A(\alpha, \xi) &= \left\{ \frac{\alpha}{6\pi^2}\left(1 - \alpha I^{(2)}\right) + \alpha^2 I^{(3)} I^{(4)} \right\} \left\{ 1 - \alpha I^{(2)} - \alpha^2 I^{(1)} I^{(4)} \right\}^{-1}, \\
\eta_\psi(\alpha, \xi) &= \alpha \cdot \left\{ I^{(3)} + \frac{\alpha}{6\pi^2} I^{(1)} \right\} \left\{ 1 - \alpha I^{(2)} - \alpha^2 I^{(1)} I^{(4)} \right\}^{-1},
\end{aligned} \tag{62}$$

where

$$\begin{aligned}
I^{(1)}(\alpha, \xi) &= \frac{1}{32\pi^2} \int_0^\infty dx x K\bar{K} \left\{ 3xK'T^2 - \xi\left(xK' + 2\bar{K}\right) L^2 \right\}, \\
I^{(2)}(\alpha, \xi) &= -\frac{1}{32\pi^2} \int_0^\infty dx \bar{K} \left\{ 3xK'(\bar{K} - K)T + \xi\left[2K\bar{K} - xK'(\bar{K} - K)\right] L \right\}, \\
I^{(3)}(\alpha, \xi) &= \frac{1}{16\pi^2} \int_0^\infty dx \left\{ x^2 K'\left[3xK'T^2 - \xi\left(xK' + 2\bar{K}\right) L^2\right] \right. \\
&\qquad \left. - x\bar{K}\left[3(K' + xK'')T + \xi(K' - xK'')L\right] \right\}, \\
I^{(4)} &= -\frac{1}{6\pi^2} \int_0^\infty dx \frac{K\bar{K}}{x}\left(\bar{K} + xK' + x^2 K''\right).
\end{aligned} \tag{63}$$

Equations (62) and (63) are written for a generic regularization function $K(x)$. Note that the integrands on the right-hand side of Eq. (63), except that for $I^{(4)}$, depend on α and ξ through $T(\alpha, x)$ and $L(\alpha, x, \xi)$, which are defined as per Eq. (32) with the quantum corrections (57).

As a result of the renormalization, we obtained nonperturbative expressions of the anomalous dimensions (62) to be used for flow equations. In the lowest order in α, Eqs. (62) become

$$\eta_A = \frac{\alpha}{6\pi^2}, \qquad \eta_\psi = \alpha I^{(3)}(0, \xi) = \frac{\alpha}{8\pi^2}\xi, \tag{64}$$

which are consistent with the known perturbative calculations.

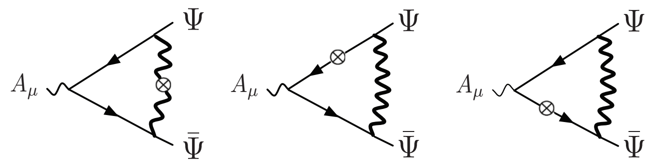

Fig. 5. The e^3 contribution to the flow of the gauge coupling. The regulator denoted by $\otimes$ is inserted in each internal line. All three diagrams contribute to the flow equation for α.

4.4. *Flows of couplings*

The RG-improved one-loop diagrams that contribute to the flow of the gauge coupling may be obtained in reference to Fig. 2. The regulator function $\otimes = \partial_t \mathcal{R} - \eta \mathcal{R}$ in Eq. (51) is to be inserted into each of the internal lines in Fig. 2. For example, the e^3-contribution consists of the three diagrams shown in Fig. 5. Similarly, we take account of diagrams with the regulator function inserted in the other eG-diagram in Fig. 2(b). The diagrams that contribute to the flow of the four-Fermi couplings are similarly constructed from Fig. 3.

The quantum corrections to the photon propagators are taken up including the momentum-dependent parts. For the fermion, we only include quantum corrections proportional to the free propagator that generate the wave function renormalization Z_2. In writing the dimensionless flow equation given in Eq. (51), we extracted out Z_2 and the internal fermion lines become the free propagators.

Finally we obtain the following flow equations for the couplings,

$$
\begin{aligned}
\partial_t \alpha &= \left(\eta_A + 2\eta_\psi\right)\alpha + \frac{\alpha\left(G_S - 4G_V\right)}{4\pi^2}\int_0^\infty dxK\bar{K}\mathcal{K}_\psi \\
&\quad + \frac{\alpha^2}{8\pi^2}\xi\int_0^\infty dx\, K\bar{K}^2\left(x\mathcal{K}_A L^2 + 2\mathcal{K}_\psi L\right), \\
\partial_t G_S &= 2(1+\eta_\psi)G_S + \frac{\left(3G_S - 8G_V\right)G_S}{8\pi^2}\int_0^\infty dxK\bar{K}\mathcal{K}_\psi \\
&\quad + \frac{\alpha G_S}{8\pi^2}\int_0^\infty dxK\bar{K}^2\left(x\mathcal{K}_A(3T^2 + \xi L^2) + 2\mathcal{K}_\psi(3T + \xi L)\right) \\
&\quad + \frac{3\alpha^2}{8\pi^2}\int_0^\infty dxK\bar{K}^3\left(x\mathcal{K}_A T^3 + \mathcal{K}_\psi T^2\right), \\
\partial_t G_V &= 2(1+\eta_\psi)G_V - \frac{G_S^2}{16\pi^2}\int_0^\infty dxK\bar{K}\mathcal{K}_\psi \\
&\quad - \frac{\alpha G_V}{8\pi^2}\int_0^\infty dxK\bar{K}^2\left(x\mathcal{K}_A(3T^2 - \xi L^2) + 2\mathcal{K}_\psi(3T - \xi L)\right) \\
&\quad + \frac{3\alpha^2}{16\pi^2}\int_0^\infty dxK\bar{K}^3\left(x\mathcal{K}_A T^3 + \mathcal{K}_\psi T^2\right),
\end{aligned}
\tag{65}
$$

where

$$
\mathcal{K}_{A(\psi)}(x;\alpha,\xi) \equiv \eta_{A(\psi)}(\alpha,\xi)\bar{K}(x) + 2xK'(x)/K(x)\,. \tag{66}
$$

Again, Eqs. (65) are written for a generic regularization function $K(x)$. For our numerical calculations to be explained shortly, we choose $K(x) = e^{-x}$.

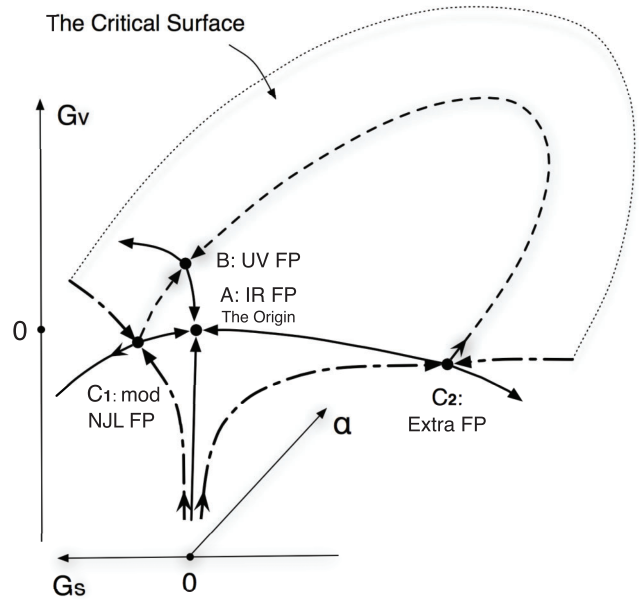

Fig. 6. Fixed points, critical surface, and critical lines. Three fixed points, A, C_1, and C_2, are located on the $\alpha = 0$ plane. The UV fixed point B has a nonzero value of $\alpha \sim 13.5$.

Table 1. Properties of four fixed points in the Landau gauge.

Fixed point	(α, G_S, G_V)	# of relevant operators
A: IR	The origin	0
B: UV	(13.5, 6.99, 0.573)	1
C_1: mod. NJL	(0, 26.3, −3.29)	2
C_2: extra	(0, −105, −52.6)	2

In Section 4.3, we obtained the photon two-point function as per Eq. (57) from the flow Eq. (51) at the lowest order of the gauge coupling. The results are consistent with the requirement $\Sigma^{AC} = 0$ by choosing the integration constants c_T as per Eq. (60) and $c_L = 0$.

In Section 3.3, we observed that the condition $\Sigma^{\bar{\Psi}\Psi C} = 0$ relates the quantum corrections $\Gamma_{\mathrm{q}}^{\bar{\Psi}\Psi}$ and $\Gamma_{\mathrm{q}}^{\bar{\Psi}A\Psi}$ with their momentum dependence. However, the ansatz (55) does not allow the momentum-dependent functions $\Gamma_{\mathrm{q}}^{\bar{\Psi}\Psi}$ and $\Gamma_{\mathrm{q}}^{\bar{\Psi}A\Psi}$ and the flow equation with the ansatz picks up only their momentum-independent contributions to give rise to the wave function renormalization for the fermion and the flow equations for couplings (65). Therefore, with the present ansatz, we do not have the same condition $\Sigma^{\bar{\Psi}\Psi C} = 0$ as in Section 3.3.

4.5. *The hierarchical phase structure*

We first present our numerical results in the Landau gauge. Figure 6 shows the phase structure obtained from the flow Eq. (65). Four fixed points are found: Their properties are listed in Table 1.

Three fixed points, A, C_1, and C_2, are located on the $\alpha = 0$ plane. The point A is the origin, the IR fixed point. C_1 is the NJL fixed point modified due to the included vector four-Fermi coupling G_V. C_2 is usually regarded as an artifact owing to the truncation of the ac-

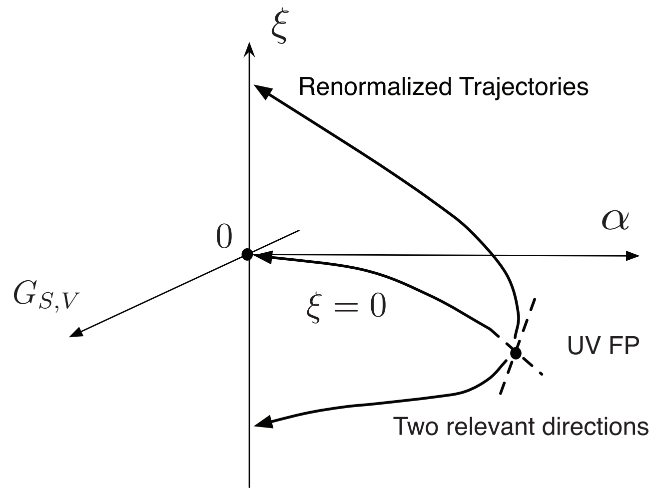

Fig. 7. Flows including that of ξ. There appears an extra relevant direction at the UV fixed point that generates flows in general gauges.

tion and ignored as an unphysical fixed point. We view it as an extra fixed point and included it since the hierarchical phase structure is better viewed with its presence. The fourth and most important fixed point, B, is found with $\alpha \neq 0$. The structure of flows around A and C_1 in the $\alpha = 0$ plane is well known, and those around C_2 turned out to be copies of those around C_1.

We proceed with a discussion of the 3D phase structure. The point A is the IR fixed point. In general, the boundary of its realm forms a 2D surface, the critical surface. It was found to be in the shape of a funnel halved by the $\alpha = 0$ plane. The densely dotted line in Fig. 6 is drawn only for the purpose of clearly showing the halved funnel. Flows restricted on the critical surface run toward the fixed point B, which has one relevant direction flowing out of the critical surface. The realm of the fixed point B for flows on the critical surface has its 1D boundaries. They are sections of the critical surface shaped in a funnel by the $\alpha = 0$ plane, i.e. two dash-dotted lines passing through C_1 and C_2.

All the flows on these two lines go into either C_1 or C_2. In 3D space, C_1 and C_2 are fixed points with two relevant directions.

Here we clearly observe a hierarchical phase structure, and the flow from B to A is the RT.

In the last column of Table 1, we list the numbers of the relevant operators. They take negative values due to our choice of the parameter $t = \ln \Lambda/\mu$.

The order $O(\alpha)$ correction $\Gamma^{AA}_{e^2}$ contributes to the photon propagator as per Eq. (32) that appears on the right-hand side of the flow equations in Eq. (65). Without the quantum correction $\Gamma^{AA}_{e^2}$, the functions T and L are simply $1/x$ and the UV fixed point is found at $(\alpha, G_S, G_V) = (13.8,\ 8.17,\ 0.578)$: The values of α and G_S differ by approximately 2.5% and 10% from those in Table 1.

We also studied flows of couplings in Eq. (65) together with the flow equation for the gauge parameter ξ given as per Eq. (61). By solving four flow equations, we found that point B in Table 1 is the unique UV fixed point. The linear analysis around B including Eq. (61) gives us two relevant directions around the UV fixed point. Numerically solving the four flow equations, we understand that the new relevant direction produces flows for gauges with $\xi \neq 0$ as depicted in Fig. 7.

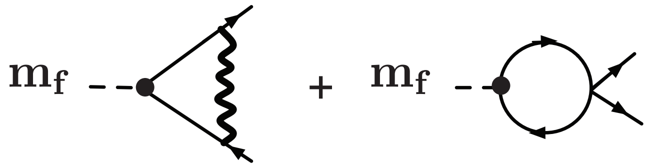

Fig. 8. Contributions to the mass anomalous dimension. Blobs indicate the $m_f\bar{\psi}\psi$ operator. To obtain γ_m, the regulator $\partial\mathcal{R}-\eta\mathcal{R}$ in Eq. (51) should be inserted into the internal propagators in these diagrams.

4.6. *Anomalous mass dimension at the UV fixed point*

The renormalization flow equations for the present system were studied earlier in Ref. [28] with other regularization functions and approximation. The UV fixed point is identified in accordance with works using the Schwinger–Dyson equations. Here we would like to calculate the anomalous mass dimension and compare the result to that obtained in Ref. [28].

Adding the mass operator $m_f\bar{\psi}\psi$ to $\Gamma_{I,\Lambda}$, we define the anomalous mass dimension γ_m by the following flow equation:

$$\partial_t m_f = -(1+\gamma_m)m_f + O(m_f^3)\,. \tag{67}$$

In calculating γ_m with the flow Eq. (51), contributions are found from the two diagrams shown in Fig. 8. In evaluating the diagrams, we insert the regulator $\partial\mathcal{R}-\eta\mathcal{R}$ in Eq. (51) into each one of the internal propagators and sum up all possible insertions. We obtain

$$\begin{aligned}\gamma_m(\alpha, G_S, \xi) = -\eta_\psi + \frac{3G_S}{4\pi^2}\left(1-\frac{2}{9}\eta_\psi\right)\\ -\frac{\alpha}{(4\pi)^2}\int_0^\infty dxK\bar{K}^2\left[x\mathcal{K}_A(3T^2+\xi L^2)+2\mathcal{K}_\psi(3T+\xi L)\right].\end{aligned} \tag{68}$$

Note that γ_m in Eq. (68) does not depend on G_V. Evaluating Eq. (68) at the UV fixed point, we find $\gamma_m = 1.078$, which is to be compared to 1.177 in Ref. [28]. At the modified NJL fixed point, $G_S^*(\alpha=0) = 8\pi^2/3$ and $\gamma_m(\alpha=0)=2$ in agreement with that of Ref. [28].

5. Gauge consistency

In Section 3, we have shown the QMEs $\Sigma^{AC} = \Sigma^{\bar{\Psi}\Psi C} = 0$ for constant gauge and four-Fermi couplings. These are results of the cancellation between the antibracket terms and the measure terms in Eqs. (39) and (45).

5.1. *QME and renormalization*

In this subsection, we consider the QME in terms of the renormalized quantities. The key observation here is the fact the couplings of Γ_e in Eq. (22) behave differently under renormalization. Note that there are no genuine quantum corrections to the second and third terms of Γ_e and the renormalization of the ghost is the only source of the change of those terms. In terms of renormalized quantities Γ_e now becomes

$$\Gamma_e = -e_{(r)}\bar{\Psi}_{(r)}\not{A}_{(r)}\Psi_{(r)} - ie'_{(r)}\Psi^*_{(r)}\Psi_{(r)}C_{(r)} + ie'_{(r)}\bar{\Psi}^*_{(r)}\bar{\Psi}_{(r)}C_{(r)}\,, \tag{69}$$

where

$$e'_{(r)} = Z_3^{-1/2}e\,. \tag{70}$$

The difference of two couplings is given as

$$e_{(r)} - e'_{(r)} = e_{(r)}[1-(Z_eZ_3^{1/2})^{-1}]\,. \tag{71}$$

It has been shown in Ref. [19] that $(Z_e Z_3^{1/2}) - 1 \propto G_{(r)S} - 4G_{(r)V}$ in the one-loop perturbative calculation. Including contributions in higher order in $e_{(r)}$, we are led to $(Z_e Z_3^{1/2}) - 1 \sim \mathcal{O}(e_{(r)}^2, G_{(r)S,V})$.

Let us find the implications of the above observation. We have shown in Section 3 that $\Sigma_e^{\bar\Psi\Psi C}$, $\Sigma_{e^2}^{AC}$, $\Sigma_{e^3}^{\bar\Psi\Psi C}$, and $\Sigma_{e\mathrm{G}}^{\bar\Psi\Psi C}$ vanish. Revisiting these calculations, we notice that $e'_{(r)}$ could appear in measure terms as well as the transformation of the fermion. Thus, we conclude that all the four Σs listed above are proportional to $e_{(r)} - e'_{(r)}$ by repeating the calculations in Section 3 using Eq. (69). Here, as the simplest example, we take the BRST transformation of the tree-level action $\bar\Psi_{(r)}(i\partial\!\!\!/ - e_{(r)}A\!\!\!/_{(r)})\Psi_{(r)}$ and find

$$\Sigma_e^{\bar\Psi\Psi C} = ie_{(r)}[1 - (Z_e Z_3^{1/2})^{-1}] \int_{p,q} \bar\Psi_{(r)}(-q)(p\!\!\!/ - q\!\!\!/)C_{(r)}(q-p)\Psi_{(r)}(p)\,. \tag{72}$$

Similarly, we find

$$\Sigma_{e^2}^{AC} \propto e_{(r)}(e_{(r)} - e'_{(r)})\,, \qquad \Sigma_{e^3}^{\bar\Psi\Psi C} \propto e_{(r)}^2(e_{(r)} - e'_{(r)})\,, \qquad \Sigma_{eG}^{\bar\Psi\Psi C} \propto G_{(r)S,V}(e_{(r)} - e'_{(r)}). \tag{73}$$

In the one-loop perturbative calculation, $e_{(r)} = e'_{(r)}$ in the absence of the four-Fermi couplings and all the Σs vanish after being written with renormalized quantities. Even in the presence of four-Fermi couplings, each Σ listed above in Eqs. (72) and (73) vanishes in the lowest order in couplings.

One may consider the possibility that the higher-order terms due to the difference of $e_{(r)}$ and $e'_{(r)}$ may cancel each other in the sum $\Sigma_e^{\bar\Psi\Psi C} + \Sigma_{e^3}^{\bar\Psi\Psi C} + \Sigma_{eG}^{\bar\Psi\Psi C}$. However, each term of the sum has a distinctive integral form owing to its Feynman graphical origin and the expected cancellation seems unlikely. This also tells us that we cannot extract any constraints among the couplings from the above sum of Σ.

We close this discussion by summarizing our findings: We have shown in Section 3 that Σ^{AC} and $\Sigma^{\bar\Psi\Psi C}$ vanish with the RG-improved one-loop contributions to the 1PI effective action. This does not produce any constraints among the couplings. When repeating the calculations using the one-loop renormalized quantities, Σ^{AC} and $\Sigma^{\bar\Psi\Psi C}$ vanish if we consider only the gauge coupling. In the presence of the four-Fermi couplings, they vanish only in the lowest power of the couplings and the higher-order corrections remain. Though we naturally expect even these higher-order corrections to Σ^{AC} and $\Sigma^{\bar\Psi\Psi C}$ to vanish, further work is required for a resolution of this intricacy.

6. Summary and discussions

We chose our 1PI effective action (26), as a nonperturbative extension of Ref. [19], based on the loop expansion in referring to the flow equation. For its construction, we made an observation that the measure contribution to the QME only has fermion loops owing to linear gauge symmetry in QED: The vertices $\Gamma_{I*}^{(2)}$ in Eq. (8) have spinor indices only as seen in Appendix A. This structure allows us to replace the IR-regulated free photon propagator with a generic one in the QME. For consistency with the flow equation, we took the photon propagator $\bar\Delta_{\mu\nu}$ with the lowest-order correction $\Gamma_{e^2}^{AA}$ to the photon two-point function. The quantum part of our 1PI effective action consists of an expansion of $\mathrm{Str}\log[(\Gamma_{\mathrm{cl}} + \Gamma_{\mathrm{q}}^{AA})^{(2)} + \mathcal{R}]$, the RG-improved one-loop formula. That is an extension of the one-loop formula $\mathrm{Str}\log[\Gamma_{\mathrm{cl}}^{(2)} + \mathcal{R}]$ which generates $\Gamma_{e^2}^{AA}$. The 1PI effective action constructed in this way simultaneously solves the flow equation and QME in approximations explained in Section 2.1. Note that the exact cancellation between the antibracket term and measure term in the QME occurs for the constant couplings.

Secondly, we introduced wave function renormalization factors Z and running couplings to obtain the flow equations with anomalous dimensions. We noticed that special attention was necessary in writing the QME in terms of the renormalized quantities.

The same constant coupling e appears both in the gauge interaction and in the BRST transformation of the fermion fields. If we could replace e by the renormalized one $e_r = Z_e e$ in both terms, the QME holds trivially. However, with the one-loop perturbative calculation, we found that the two terms are renormalized differently: The BRST transformation of the fermion field acquires the coefficient $e'_r = e_r/(Z_e Z_3^{1/2})$. As discussed in Section 5, this makes the quantum master functional proportional to $e_r - e'_r$. After the one-loop perturbative renormalization, the QME holds only approximately. We leave this question for a future study.

Thirdly, we reported our numerical study. Our ansatz contains the quantum correction to the photon two-point function that is constructed consistently with both the flow equation and QME. Based on our observation of the QME in Section 3, we used the dressed photon propagator (31) which is nonperturbative by its construction. The flow equation gave us the anomalous dimensions as per Eq. (62) which is also nonperturbative and fully utilized in our numerical study. With our ansatz and approximations, we identified the UV fixed point whose properties are consistent with earlier works.

As for the quantum corrections to the fermion two-point function and the three-point interaction vertex, only those proportional to their tree forms are included in our numerical study: Those quantum corrections give rise to the renormalization of the gauge coupling and the anomalous dimension for the fermion. Incorporating form factors similarly to the photon two-point function, we may be able to obtain the fermion two-point function and the three-point interaction vertex discussed in Section 3. Inclusion of those momentum-dependent quantum corrections is left for future research.

In Section 3, two relations out of the QME, $\Sigma^{AC} = \Sigma^{\bar{\Psi}\Psi C} = 0$, are shown to hold even with the dressed photon propagator. Using the same propagators and vertices as Section 3, we calculated the loop of the flow Eq. (51) for our numerical study. In deriving Eq. (65), we used the derivative expansion and that makes it difficult to consider $\Sigma^{\bar{\Psi}\Psi C} = 0$ explicitly in Section 4. The numerical results of Section 4 are obtained with the flow equations of couplings (65) within our approximations.

Acknowledgments

Y.I. and K.I. are grateful to J.-I. Sumi for stimulating discussions. Y.T. is grateful to M. Tanimoto and H. Nakano for their encouragements.

Funding

The work by Y.I. and K.I. has been supported in part by the Grants-in-Aid for Scientific Research nos. 19K03822 and 23K03412 from Japan Society for the Promotion of Science. This work is supported by EMMI and by ERC-AdG-290623. This work is also funded by the Deutsche Forschungsgemeinschaft (DFG, German Research Foundation) under Germany's Excellence Strategy EXC 2181/1—390900948 (the Heidelberg STRUCTURES Excellence Cluster) and the Collaborative Research Centre SFB 1225 (ISOQUANT). It is also supported by EMMI. Open Access funding: SCOAP^3.

Appendix A. Vertices

To calculate the quantum corrections Γ_q and the measure term Σ_K, we need field-dependent parts of $\Gamma_I^{(2)}$, namely the vertices $\tau[\Phi]$ defined in Eq. (12), and $\Gamma_{I*}^{(2)}$ in Eq. (9). From Γ_e in Eq. (22) we find the following vertices:

$$
\begin{aligned}
\tau_{\hat{\alpha}\beta}^{(-\not{A})}(x,y) &= \frac{\partial^l \partial^r \Gamma_e}{\partial \bar{\Psi}_{\hat{\alpha}}(x) \partial \Psi_\beta(y)} = -e(\not{A})_{\hat{\alpha}\beta}(x)\delta(x-y), \\
\tau_{\alpha\hat{\beta}}^{(\not{A}^T)}(x,y) &= \frac{\partial^l \partial^r \Gamma_e}{\partial \Psi_\alpha(x) \partial \bar{\Psi}_{\hat{\beta}}(y)} = +e(\not{A}^T)_{\alpha\hat{\beta}}(x)\delta(x-y), \\
\tau_{\hat{\alpha}\mu}^{(-\gamma\Psi)}(x,y) &= \frac{\partial^l \partial^r \Gamma_e}{\partial \bar{\Psi}_{\hat{\alpha}}(x) \partial A_\mu(y)} = -e(\gamma_\mu \Psi)_{\hat{\alpha}}(x)\delta(x-y) = -\tau_{\mu\hat{\alpha}}^{(\gamma\Psi)}(x,y), \\
\tau_{\mu\beta}^{(-\bar{\Psi}\gamma)}(x,y) &= \frac{\partial^l \partial^r \Gamma_e}{\partial A_\mu(x) \partial \Psi_\beta(y)} = -e(\bar{\Psi}\gamma_\mu)_\beta(x)\delta(x-y) = -\tau_{\beta\mu}^{(\bar{\Psi}\gamma)}(x,y).
\end{aligned}
\tag{A.1}
$$

Here the superscripts of τ indicate structures of vertices. Similarly from $\Gamma_G^{(2)}$, we have

$$
\begin{aligned}
\tau_{\hat{\alpha}\beta}^{(\bar{\Psi}\Psi)}(x,y) &= \left[\frac{\partial^l \partial^r \Gamma_G[\Phi]}{\partial \bar{\Psi}_{\hat{\alpha}}(x) \partial \Psi_\beta(y)}\right]_{A=0} \\
&= \frac{G_S}{\Lambda^2}\delta(x-y)\Big\{\big[\delta_{\hat{\alpha}\beta}(\bar{\Psi}(x)\Psi(x)) - (\gamma_5)_{\hat{\alpha}\beta}(\bar{\Psi}(x)\gamma_5\Psi(x))\big] \\
&\quad - \big[\bar{\Psi}_\beta(x)\Psi_{\hat{\alpha}}(x) - (\bar{\Psi}\gamma_5)_\beta(x)(\gamma_5\Psi)_{\hat{\alpha}}(x)\big]\Big\} \\
&\quad + \frac{G_V}{\Lambda^2}\delta(x-y)\Big\{\big[(\gamma_\mu)_{\hat{\alpha}\beta}\left(\bar{\Psi}(x)\gamma_\mu\Psi(x)\right) + (\gamma_5\gamma_\mu)_{\hat{\alpha}\beta}\left(\bar{\Psi}(x)\gamma_5\gamma_\mu\Psi(x)\right)\big] \\
&\quad - \big[\left(\bar{\Psi}(x)\gamma_\mu\right)_\beta\left(\gamma_\mu\Psi(x)\right)_{\hat{\alpha}} + \left(\bar{\Psi}(x)\gamma_5\gamma_\mu\right)_\beta\left(\gamma_5\gamma_\mu\Psi(x)\right)_{\hat{\alpha}}\big]\Big\} \\
&= -\left(\tau^{(\bar{\Psi}\Psi)}\right)^T_{\beta\hat{\alpha}}(y,x),
\end{aligned}
\tag{A.2}
$$

$$
\begin{aligned}
\tau_{\alpha\beta}^{(\bar{\Psi}\bar{\Psi})}(x,y) &= \frac{\partial^l \partial^r \Gamma_G}{\partial \Psi_\alpha(x) \partial \Psi_\beta(y)} \\
&= -G_S\delta(x-y)\big[\bar{\Psi}_\alpha(x)\bar{\Psi}_\beta(x) - (\bar{\Psi}\gamma_5)_\alpha(x)(\bar{\Psi}\gamma_5)_\beta(x)\big] \\
&\quad - G_V\delta(x-y)\big[(\bar{\Psi}\gamma_\mu)_\alpha(x)(\bar{\Psi}\gamma_\mu)_\beta(x) + (\bar{\Psi}\gamma_5\gamma_\mu)_\alpha(x)(\bar{\Psi}\gamma_5\gamma_\mu)_\beta(x)\big],
\end{aligned}
\tag{A.3}
$$

and

$$
\begin{aligned}
\tau_{\hat{\alpha}\hat{\beta}}^{(\Psi\Psi)}(x,y) &= \frac{\partial^l \partial^r \Gamma_G}{\partial \bar{\Psi}_{\hat{\alpha}}(x) \partial \bar{\Psi}_{\hat{\beta}}(y)} \\
&= -G_S\delta(x-y)\Big[\Psi_{\hat{\alpha}}(x)\Psi_{\hat{\beta}}(x) - (\gamma_5\Psi)_{\hat{\alpha}}(x)(\gamma_5\Psi)_{\hat{\beta}}(x)\Big] \\
&\quad - G_V\delta(x-y)\Big[(\gamma_\mu\Psi)_{\hat{\alpha}}(x)(\gamma_\mu\Psi)_{\hat{\beta}}(x) + (\gamma_5\gamma_\mu\Psi)_{\hat{\alpha}}(x)(\gamma_5\gamma_\mu\Psi)_{\hat{\beta}}(x)\Big].
\end{aligned}
\tag{A.4}
$$

We find $\Gamma_{I*}^{(2)}$ in Eq. (9) as

$$
\begin{aligned}
\tau_{*\alpha\beta}^{C} &= \frac{\partial}{\partial \Psi_\alpha^*(x)} \frac{\partial^r}{\partial \Psi_\beta(y)}\Gamma_e = +ie\delta_{\alpha\beta}C(x)\delta(x-y), \\
\tau_{*\hat{\alpha}\hat{\beta}}^{C} &= \frac{\partial}{\partial \bar{\Psi}_{\hat{\alpha}}^*(x)} \frac{\partial^r}{\partial \bar{\Psi}_{\hat{\beta}}(y)}\Gamma_e = -ie\delta_{\hat{\alpha}\hat{\beta}}C(x)\delta(x-y).
\end{aligned}
\tag{A.5}
$$

Appendix B. Photon two-point function and anomalous dimensions

We derive the flow equation for the photon two-point function in Eq. (56) and two relations of the anomalous dimensions to be solved as per Eq. (62).

B.1. Flow equation for photon two-point function

The flow equations for $\mathcal{A}_{\mu\nu} = P^T_{\mu\nu}\mathcal{T}(t,x) + P^L_{\mu\nu}\mathcal{L}(t,x)$ ($x = p^2$) are

$$\begin{aligned}&(\partial_t - \eta_A(t))\,\mathcal{T} - \eta_A(t)x - 2\,(x\partial_x - 1)\,\mathcal{T} = -2\alpha(t)C_T\left(\eta_\psi(t), x\right),\\ &(\partial_t - \eta_A(t))\,\mathcal{L} + x\left(\dot{\xi}(t)^{-1} - \eta_A(t)\xi(t)^{-1}\right) - 2\,(x\partial_x - 1)\,\mathcal{L} = -2\alpha(t)C_L\left(\eta_\psi(t), x\right),\end{aligned} \tag{B.1}$$

where $x = p^2$. The two coefficient functions on the r.h.s. of Eqs. (B1) are given as

$$\begin{aligned}C_T(\eta_\psi(t), x) &= \frac{4}{3}\int_k \frac{\left(K\mathcal{K}_\psi\right)(k)}{k^2}\cdot\frac{\bar{K}(p+k)}{(p+k)^2}\left(3(p\cdot k) + k^2 + \frac{2(p\cdot k)^2}{p^2}\right),\\ C_L(\eta_\psi(t), x) &= -4\int_k \frac{\left(K\mathcal{K}_\psi\right)(k)}{k^2}\cdot\frac{\bar{K}(p+k)}{(p+k)^2}\left((p\cdot k) - k^2 + \frac{2(p\cdot k)^2}{p^2}\right),\end{aligned} \tag{B.2}$$

where $\mathcal{K}_\psi$ is defined in Eq. (66) as

$$\mathcal{K}_\psi(\eta_\psi,\ x) \equiv \eta_\psi \bar{K}(x) + 2xK'(x)/K(x)\,. \tag{B.3}$$

C_T and C_L in Eqs. (B2) are functionals of the regulator function K. They depend on the scale t through $\eta_\psi(t)$.

In Eqs. (B1), x-linear terms play special roles. Let us first consider Eqs. (B1) for $\mathcal{T}$. Due to renormalization, $\mathcal{T}$ does not have any x-linear terms. In Eqs. (B1), the anomalous dimension on the l.h.s. must balance to the coefficient of the x-linear term on the r.h.s.: we find a relation of the anomalous dimensions

$$\eta_A = \frac{\alpha}{6\pi^2} + \alpha\eta_\psi I^{(4)}, \tag{B.4}$$

where

$$I^{(4)} = -\frac{1}{6\pi^2}\int_0^\infty dx\frac{K\bar{K}}{x}\left(\bar{K} + xK' + x^2K''\right). \tag{B.5}$$

In Eqs. (B1) for $\mathcal{L}$, we note terms linear in x and the vanishing of its coefficient gives rise to the flow equation for the gauge parameter:

$$\dot{\xi}(t)^{-1} = \eta_A(t)\xi(t)^{-1}\,. \tag{B.6}$$

This is consistent with Eq. (50).

It would be appropriate to explain why other terms of the second equation of Eqs. (B1) do not produce any x-linear terms: (i) As we will find in Eq. (B18), $\mathcal{L}$ vanishes for a large x and the first term on the l.h.s. does not have any x-linear terms, at least in the lowest order in α; (ii) in the third term on the l.h.s., the operator $x\partial_x - 1$ removes x-linear terms in $\mathcal{L}$; and (iii) we find that the coefficient function $C_L(\eta_\psi(t), x)$ in Eqs. (B1) does not have any x-linear terms after some calculations. Observation (ii) is trivial; let us explain the two other properties.

We start from property (iii). With the regulator function $K(x) = e^{-x}$, we may explicitly calculate the coefficient function C_L in Eqs. (B2) as

$$\begin{aligned}C_L(\eta_\psi, x) = &\frac{3}{2\pi^2x^2}\left\{1 - \frac{2x}{3} - \left(1 - \frac{x}{6} - \frac{x^2}{12}\right)e^{-x/2}\right\}\\ &+\frac{\eta_\psi}{4\pi^2x^2}\left\{-\frac{3}{4}\left(x - \frac{7}{6}\right) + (x-2)e^{-x/2} - \frac{1}{2}\left(x - \frac{9}{4}\right)e^{-2x/3}\right\},\end{aligned} \tag{B.7}$$

by using the integral representation of the modified Bessel function:

$$\int_0^\pi d\theta \exp(2pq\cos\theta)\sin^2\theta = \frac{\pi}{2pq} I_1(2pq). \tag{B.8}$$

One can confirm that there is no x-linear term in Eq. (B7) and it is easy to see that $C_L(\eta_\psi, x)$ vanishes for a large x. We have not proved this property for a generic regulator function $K(x)$.

Shortly we find the solution to Eqs. (B1) in the lowest order in α as given in Eq. (57). The solution vanishes as $1/x$ for a large x [cf. Eq. (B18)]. That implies Eq. (B6) since Eqs. (B1) are understood to hold for a generic x.

In the lowest order in α, Eqs. (B1) become

$$(x\partial_x - 1)\,\mathcal{T}(t,x) = \alpha C_T(0,x) - \frac{\alpha}{12\pi^2}, \qquad (x\partial_x - 1)\,\mathcal{L}(t,x) = \alpha C_L(0,x). \tag{B.9}$$

The coefficient functions of the r.h.s. of Eqs. (B9) are

$$\begin{aligned} C_T(0,x) &= \frac{8}{3}\int_k \frac{K'(k)\bar{K}(p+k)}{(p+k)^2}\left(3(p\cdot k) + k^2 + \frac{2(p\cdot k)^2}{p^2}\right), \\ C_L(0,x) &= -8\int_k \frac{K'(k)\bar{K}(p+k)}{(p+k)^2}\left((p\cdot k) - k^2 + \frac{2(p\cdot k)^2}{p^2}\right). \end{aligned} \tag{B.10}$$

For $K(x) = e^{-x}$, Eqs. (B9) become

$$\begin{aligned} \left(x\frac{\partial}{\partial x} - 1\right)\mathcal{T}(t,x) &= -\frac{\alpha}{8\pi^2 x^2}\left\{4 + \frac{2x^3}{3} - \left(4 + 2x - x^2\right)\exp(-x/2)\right\}, \\ \left(x\frac{\partial}{\partial x} - 1\right)\mathcal{L}(t,x) &= \frac{\alpha}{8\pi^2 x^2}\left\{12 - 8x - \left(12 - 2x - x^2\right)\exp(-x/2)\right\}. \end{aligned} \tag{B.11}$$

Solving Eqs. (B11), we obtain

$$\begin{aligned} \mathcal{T}(t,x) &= \frac{\alpha(t)}{6\pi^2 x^2}\left[1 - \left(1 + \frac{x}{2} - x^2\right)\exp(-x/2) + \frac{x^3}{2}\left(\mathrm{Ei}(-x/2) - \log x\right)\right] + c_T x, \\ \mathcal{L}(t,x) &= -\frac{\alpha(t)}{2\pi^2 x^2}\left[1 - x - \left(1 - \frac{x}{2}\right)\exp(-x/2)\right] + c_L x, \end{aligned} \tag{B.12}$$

where $\mathrm{Ei}(-x/2)$ denotes the exponential integral defined as

$$\mathrm{Ei}(-y) = \int_\infty^y \frac{e^{-u}}{u}du. \tag{B.13}$$

Note that $\mathcal{T}$ and $\mathcal{L}$ are t-dependent quantities through their dependence on $\alpha(t)$. Here, c_T and c_L are integration constants. We will explain presently that those constants are

$$c_T = \frac{1}{12\pi^2}\left(\frac{13}{12} - \gamma + \log 2\right), \qquad c_L = 0, \tag{B.14}$$

where γ is the Euler's constant that appears in the power series expansion of $\mathrm{Ei}(-x/2)$.

The transverse part $\mathcal{T}$ does not have any x-linear terms due to the renormalization: The condition determines the above value of c_T. Here we used the expansion

$$\mathrm{Ei}(-y) = \gamma + \log y + \sum_{n=1}^{\infty}\frac{(-1)^n y^n}{n!\,n}. \tag{B.15}$$

The QME $\Sigma^{AC} = 0$ can be used to determine the longitudinal part $\mathcal{L}$ as per Eq. (59). In Ref. [20], it was shown that Eq. (59) gives $\mathcal{L}(t,x)$ in Eq. (57) with $c_L = 0$ for our choice $K(x) = e^{-x}$.

Two comments are in order. For a large value of $x = p^2$, the exponential integral $\mathrm{Ei}(-x/2)$ tends to zero and we find

$$\mathcal{T}(t,x) \sim -\frac{\alpha(t)}{6\pi^2}\cdot\frac{1}{2}\cdot x\log x. \tag{B.16}$$

$\alpha(t)/(6\pi^2)$ is the anomalous dimension of the photon in the lowest order. Equation (B16) may be regarded as the lowest-order expansion of the following behavior:

$$p^2 + \mathcal{T}(t, p^2) \sim p^{2-\eta_A}\,. \tag{B.17}$$

$\mathcal{L}$ in Eq. (57) with $c_L = 0$ behaves for small and large x as

$$\mathcal{L}(t, x) \sim \frac{\alpha(t)}{2\pi^2} \times \begin{cases} 3/8 - x/12 & x \sim 0 \\ 1/x & x \sim \infty\,. \end{cases} \tag{B.18}$$

B.2. Relation between anomalous dimensions from fermion two-point function

By repeating a similar calculation for the fermion two-point function, we find the following relation among the anomalous dimensions:

$$\eta_\psi = \alpha\left(\eta_A I^{(1)} + \eta_\psi I^{(2)} + I^{(3)}\right). \tag{B.19}$$

Solving Eqs. (B4) and (B19) for η_A and η_ψ, we obtain Eq. (62).

Appendix C. Gauge-consistent fRG expansion scheme

In this appendix we augment the explicit derivations in this work with a more structural point of view on our approach. This is specifically important for potential systematic improvements of the approach. We may split the workflow into two structural parts.

(1) Construct a gauge-consistent approximation Γ_{gc} to the effective action. This approximation is given in terms of the effective action itself and its derivatives, see e.g. Eq. (2) or Eq. (C2a) in Appendix C.1 below.

(2) Derive flow equations for the gauge-consistent couplings of Γ_{gc} within a respective approximation of the flow equation. For a structural point of view see Appendix C.2.

The second step will be discussed in Appendix C.2 where we show that the 1PI effective action with the the RG-improved formula (2) can be understood as an approximate solution to the flow equation with a particular set of interaction vertices. Put differently, we show how the flow of the vertices of Eq. (2) is computed from the flow equation.

C.1. Systematic skeleton expansion scheme

We start our analysis with restructuring the Wetterich Eq. (10) as a total derivative and RG-improvement terms,

$$\partial_t \Gamma = \frac{1}{2}\text{Str}\frac{1}{\Gamma^{(2)} + \mathcal{R}}\partial_t \mathcal{R} = \frac{1}{2}\text{Str}\,\partial_t \ln\left[\Gamma^{(2)} + \mathcal{R}\right] - \frac{1}{2}\text{Str}\frac{1}{\Gamma^{(2)} + \mathcal{R}}\partial_t \Gamma^{(2)}\,. \tag{C.1}$$

Upon t-integration from the initial cutoff scale t_0 to t, Eq. (C1) gives us,

$$\Gamma(t) = \Gamma^1_{\text{sk}}(t) - \frac{1}{2}\int_{t_0}^{t} dt'\,\text{Str}\frac{1}{(\Gamma^{(2)} + \mathcal{R})(t')}\partial_{t'}\Gamma^{(2)}(t')\,, \tag{C.2a}$$

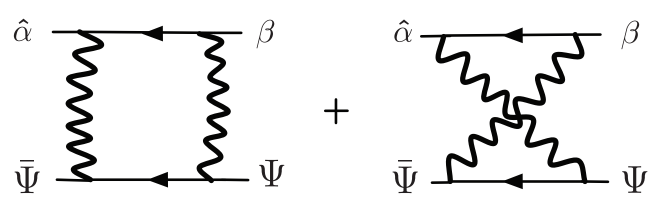

Fig. C1. $\left(\tau^{\bar{\Psi}\Psi}_{e^4}\right)_{\hat{\alpha}\beta}$ in Eq. (C13).

with the first-order $\Gamma^1_{\rm sk}(t)$ of the skeleton expansion in the presence of the regulator,

$$\Gamma^1_{\rm sk}(t) = \Gamma(t_0) + \frac{1}{2}\mathrm{Str}\left(\ln\left[\Gamma^{(2)} + \mathcal{R}\right](t) - \ln\left[\Gamma^{(2)} + \mathcal{R}\right](t_0)\right)\,, \tag{C.2b}$$

the effective action in Eq. (2). The structure of Eq. (C2a) is that of a one-loop functional of the full second derivative of the effective action, $\Gamma^{(2)}$, and an RG-improvement term. This term can be rewritten as a two-loop functional in terms of $\Gamma^{(2)}$ similarly to Eq. (C2b), and a higher-order RG-improvement term. For the sake of illustration we indicate this procedure with the next order. In a first step we use the skeleton expansion (C2) for the flow of $\Gamma^{(2)}$. This results in

$$\partial_t\Gamma^{(2)} = \tfrac{1}{2}\mathrm{Str}\,\partial_t\left[\tfrac{1}{\Gamma^{(2)}+\mathcal{R}}\left(\Gamma^{(4)} - \Gamma^{(3)}\tfrac{1}{\Gamma^{(2)}+\mathcal{R}}\Gamma^{(3)}\right)\right] - \tfrac{1}{2}\mathrm{Str}\left[\tfrac{1}{\Gamma^{(2)}+\mathcal{R}}\partial_t\Gamma^{(2)}\right]^{(2)}. \tag{C.3}$$

The last comprises second-order terms in the skeleton expansion, which only contribute to third-order ones if Eq. (C3) is inserted in the last term of Eq. (C2a): They give rise to integrated two-loop terms similar to that in Eq. (C2a). As $\partial_t\Gamma^{(2)}$ is given by a skeleton loop itself, it is at least third order in the skeleton expansion.

The first term on the r.h.s. of Eq. (C3) is a total derivative. If inserted into the integrand in the last term in Eq. (C2a), the integrand can be written as a total derivative and higher-order terms. We find

$$\frac{1}{2}\mathrm{Str}\frac{1}{\Gamma^{(2)}+\mathcal{R}}\partial_t\Gamma^{(2)} = \partial_t\left[\frac{1}{4}\frac{1}{\Gamma^{(2)}+\mathcal{R}}\Gamma^{(4)}\frac{1}{\Gamma^{(2)}+\mathcal{R}} - \frac{1}{6}\Gamma^{(3)}\left(\frac{1}{\Gamma^{(2)}+\mathcal{R}}\right)^3\Gamma^{(3)}\right]$$
$$+3\text{rd-order terms}, \tag{C.4}$$

where all propagators are fully contracted with the vertices. In the second term all propagators are contracted with both vertices. Upon integration the first term provides the second-order skeleton terms and higher-order terms. For the second-order terms we can choose a gauge-consistent approximation for $\Gamma^{(n)}$, thereby solving the QME. We shall discuss this explicitly for the first order used in the present work in Appendix C.2.

Finally we remark that this procedure can be iterated systematically. In summary, the general gauge-consistent procedure discussed in the present work is now implemented as follows: First we observe that the QME connects different orders in the skeleton expansion. Still we reduce Eq. (C2a) to its first-order contribution and implement a gauge-consistent approximation to $\Gamma^1_{\rm sk}$ in terms of a respective approximation of $\Gamma^{(2)}$. Diagrams derived from Eq. (C2b) are the one-loop diagrams (lowest order) in the full propagators and vertices in a skeleton expansion. In Appendix C.2 we shall discuss the gauge consistency of Eq. (C2b) with an appropriate approximation for $\Gamma^{(2)}$.

C.2. Flow equation for the RG-improved action

Before looking into the RG-improved formula in Eq. (2), let us first consider the standard one-loop approximation in Eq. (1). This formula is obtained by putting only the classical interaction action $\Gamma_{I,\rm cl}$ on the r.h.s. of the flow equation at all the scale t: all the accumulating quantum contributions are ignored at every step of solving the flow equation. Similarly we will presently find that the RG-improved formula (2) is obtained collecting a particular set of quantum corrections.

Suppose now we have the action with Eq. (2) added to the classical action at a scale t:

$$\Gamma_I(t) = \Gamma_{I,\rm cl} + \frac{1}{2}\mathrm{Str}\log\left[(\Gamma_{\rm cl} + \Gamma_{\rm q}^{AA})^{(2)} + \mathcal{R}\right](t)\,. \tag{C.5}$$

The second term on the r.h.s. of Eq. (C5) generates terms in Eq. (33) with the classical vertices, the tree fermion, and the dressed photon propagators.

The condition that $\Gamma_I(t+\Delta t)$ generated as per Eq. (16) is also given by the formula in Eq. (C5) is expressed as

$$\frac{d}{dt}\mathrm{Str}\log\left[(\Gamma_{\rm cl}+\Gamma_{\rm q}^{AA})^{(2)}+\mathcal{R}\right](t) = \frac{1}{2}\mathrm{Str}\left[\otimes\frac{1}{\bar{\Delta}^{-1}+\tau[\Phi]}\right](t)\,. \tag{C.6}$$

$\bar{\Delta}^{-1}$ and $\tau[\Phi]$ are defined at the scale t as per Eqs. (13) and (12). Equation (C5) satisfies the flow equation with some approximations and we will explain how Eq. (C6) holds by taking appropriate vertices for $\tau[\Phi]$ on the r.h.s.

The expansion of the RG-improved formula is given in Eq. (33) as

$$\mathrm{Str}\log\left[(\Gamma_{\rm cl}+\Gamma_{\rm q}^{AA})^{(2)}+\mathcal{R}\right] = \Gamma_{e^2}^{AA}+\Gamma_{e^2}^{\bar{\Psi}\Psi}+\Gamma_{\rm q}^{\bar{\Psi}A\Psi}+\Gamma_{\rm q}^{\bar{\Psi}\Psi\bar{\Psi}\Psi}+\cdots\,. \tag{C.7}$$

The first term $\Gamma_{e^2}^{AA}$ consists of a fermion one-loop. For this term (C6) is satisfied with the classical vertices $\tau_{\rm cl}$, the 3-point vertices $\tau^{(-\not{A})}$ and $\tau^{(\not{A}^T)}$ given in Eq. (A1). Similarly, for terms in Eq. (C7) only with fermion internal lines, we need the classical vertices to satisfy Eq. (C6).

The second term $\Gamma_{e^2}^{\bar{\Psi}\Psi}$ contains a fermion and a dressed photon propagator. Taking its derivative, we find

$$\dot{\Gamma}_{\rm e^2}^{\bar{\Psi}\Psi} = -e^2\bar{\Psi}\gamma_\mu\left(\dot{\bar{\Delta}}^{(0)}\gamma_\nu\bar{\Delta}_{\mu\nu}+\bar{\Delta}^{(0)}\gamma_\nu\dot{\bar{\Delta}}_{\mu\nu}\right)\Psi\,. \tag{C.8}$$

The derivative of the dressed photon propagator acts on $\mathcal{A}$ as well as the regulator $\mathcal{R}$,

$$\partial_t\bar{\Delta}_{\mu\nu} = -\left(\bar{\Delta}\partial_t[(\bar{\Delta}^{(0)})^{-1}+\mathcal{A}]\bar{\Delta}\right)_{\mu\nu} = -\left(\bar{\Delta}[\dot{\mathcal{R}}+\dot{\mathcal{A}}]\bar{\Delta}\right)_{\mu\nu}\,. \tag{C.9}$$

$\mathcal{R}$ is the regulator defined in Eq. (11) and its derivative is

$$\dot{\mathcal{R}} = \otimes = -(\bar{\Delta}^{(0)})^{-1}\dot{\bar{\Delta}}^{(0)}(\bar{\Delta}^{(0)})^{-1}\,. \tag{C.10}$$

The flow of $\Gamma_{\rm e^2}^{\bar{\Psi}\Psi}$ is given by

$$\begin{aligned}\dot{\Gamma}_{\rm e^2}^{\bar{\Psi}\Psi} &= e^2\bar{\Psi}\gamma_\mu\left[\left(\bar{\Delta}^{(0)}\dot{\mathcal{R}}\bar{\Delta}^{(0)}\right)\gamma_\nu\bar{\Delta}_{\mu\nu}+\bar{\Delta}^{(0)}\gamma_\nu\left(\bar{\Delta}\dot{\mathcal{R}}\bar{\Delta}\right)_{\mu\nu}\right]\Psi\\ &\quad+e^2\left(\bar{\Psi}\gamma_\mu\bar{\Delta}^{(0)}\gamma_\nu\Psi\right)\left(\bar{\Delta}\dot{\mathcal{A}}\bar{\Delta}\right)_{\mu\nu}\,.\end{aligned} \tag{C.11}$$

The terms on the first line of the r.h.s. of Eq. (C11) are in the expected RG-improved one-loop form with $\tau_{\rm cl}$, whereas the last term is obviously in two-loop form. We will show that this term may also be rewritten in the form of the l.h.s. of Eq. (C6) with an appropriate vertex $\tau[\Phi]$.

Using $\mathcal{A}_{\rho\sigma}$ given in Eq. (34),

$$\mathcal{A}_{\rho\sigma} = \frac{e^2}{2}\mathrm{tr}\left(\bar{\Delta}^{(0)}\gamma_\rho\bar{\Delta}^{(0)}\gamma_\sigma\right), \tag{C.12}$$

we find the second term in Eq. (C11) as

$$\begin{aligned}&e^2\left(\bar{\Psi}\gamma_\mu\bar{\Delta}^{(0)}\gamma_\nu\Psi\right)\left(\bar{\Delta}\dot{\mathcal{A}}\bar{\Delta}\right)_{\mu\nu}\\ &= e^2\left(\bar{\Psi}\gamma_\mu\bar{\Delta}^{(0)}\gamma_\nu\Psi\right)\bar{\Delta}_{\mu\rho}\bar{\Delta}_{\nu\sigma}\cdot\frac{e^2}{2}\left[\mathrm{tr}\left(\dot{\bar{\Delta}}^{(0)}\gamma_\rho\bar{\Delta}^{(0)}\gamma_\sigma\right)+\mathrm{tr}\left(\bar{\Delta}^{(0)}\gamma_\rho\dot{\bar{\Delta}}^{(0)}\gamma_\sigma\right)\right]\\ &= -\frac{1}{2}\mathrm{tr}\left(\otimes\bar{\Delta}^{(0)}\tau_{e^4}^{\bar{\Psi}\Psi}\bar{\Delta}^{(0)}\right).\end{aligned} \tag{C.13}$$

Here $\left(\tau_{e^4}^{\bar{\Psi}\Psi}\right)_{\hat{\alpha}\beta}$ represents a pair of vertices shown in Fig. C1 obtained from $\Gamma_{e^4}^{\bar{\Psi}\Psi\bar{\Psi}\Psi}$ in Fig. 3(a) and 3(b). The expression in Eq. (C13) is a fermion one-loop with the vertex $\tau_{e^4}^{\bar{\Psi}\Psi}$ and the regulator inserted: It is the expected one-loop form on the l.h.s. of Eq. (C6). The vertex $\Gamma_{\rm e^2}^{\bar{\Psi}\Psi}$ has a dressed photon propagator and the scale change also acts on $\mathcal{A}_{\mu\nu}$ in the propagator. Still, we have shown that all the terms of $\dot{\Gamma}^{\bar{\Psi}\Psi}_{e^2}$ in Eq. (C8) are expressed as one-loop forms on the l.h.s. of Eq. (C6).

We also studied $\Gamma^{\bar{\Psi}A\Psi}_{e^3}$, which also has a dressed photon propagator, and confirmed that all the terms in the scale derivative of the vertex are expressed in one-loop forms on the l.h.s. of Eq. (C6) by including appropriate RG-improved one-loop vertices.

In the above, we have explained that Eq. (C6) holds for the first three terms in the expansion Eq. (C7). Though we have not proved that arguments similar to the above apply to all the terms in the expansion (C7), the above results imply strongly that $\Gamma_I(t)$ in Eq. (C5) satisfies the flow equation with the classical vertices $\tau_{\rm cl}$ and appropriate RG-improved one-loop vertices.

C.3. On the dimensionless flow equation

The flow Eq. (51) in the dimensionless form collects quantum corrections in a different manner from that explained above. To point out the difference is the purpose of this subsection.

By putting an ansatz on the r.h.s. of the flow equation, we add higher-order quantum corrections that make the action different from the original ansatz. Using a derivative expansion, we reduce the resultant action into the form of our ansatz but with different couplings. The renormalization with the Z factors is introduced in this step and we find the flow equations of the couplings. The process of accumulating higher-order quantum corrections defines the non-perturbative runnings of the couplings though the form of the 1PI action is always kept in the form of a chosen ansatz. This is the approximation for the flow Eq. (51) to obtain Eq. (65).

REFERENCES

[1] Y. Igarashi, K. Itoh, and H. So, Prog. Theor. Phys. **104**, 1053 (2000) [arXiv:hep-th/0006180] [Search inSPIRE].
[2] Y. Igarashi, K. Itoh, and H. So, Prog. Theor. Phys. **106**, 149 (2001) [arXiv:hep-th/0101101] [Search inSPIRE].
[3] Y. Igarashi, K. Itoh, and H. Sonoda, Prog. Theor. Phys. **118**, 121 (2007) [arXiv:0704.2349 [hep-th]] [Search inSPIRE].
[4] T. Higashi, E. Itou, and T. Kugo, Prog. Theor. Phys. **118**, 1115 (2007) [arXiv:0709.1522 [hep-th]] [Search inSPIRE].
[5] I. A. Batalin and G. A. Vilkovisky, Phys. Lett. B **102**, 27 (1981).
[6] W.-j. Fu, Commun. Theor. Phys. **74**, 097304 (2022) [arXiv:2205.00468 [hep-ph]] [Search inSPIRE].
[7] N. Dupuis, L. Canet, A. Eichhorn, W. Metzner, J. M. Pawlowski, M. Tissier, and N. Wschebor, Phys. Rept. **910**, 1 (2021) [arXiv:2006.04853 [cond-mat.stat-mech]] [Search inSPIRE].
[8] J. Braun, J. Phys. G **39**, 033001 (2012) [arXiv:1108.4449 [hep-ph]] [Search inSPIRE].
[9] O. J. Rosten, Phys. Rept. **511**, 177 (2012) [arXiv:1003.1366 [hep-th]] [Search inSPIRE].
[10] Y. Igarashi, K. Itoh, and H. Sonoda, Prog. Theor. Phys. Suppl. **181**, 1 (2010) [arXiv:0909.0327 [hep-th]] [Search inSPIRE].
[11] H. Gies, Lect. Notes Phys. **852**, 287 (2012) [arXiv:hep-ph/0611146] [Search inSPIRE].
[12] J. M. Pawlowski, Ann. Phys. **322**, 2831 (2007) [arXiv:hep-th/0512261] [Search inSPIRE].
[13] C. Bambi, L. Modesto, and I. Shapiro, Handbook of Quantum Gravity (Springer, Singapore, 2024).
[14] J. M. Pawlowski and M. Reichert, Front. Phys. **8**, 551848 (2021) [arXiv:2007.10353 [hep-th]] [Search inSPIRE].
[15] F. Ihssen and J. M. Pawlowski, Phys. Rev. D **112**, 105005 (2025) [arXiv:2503.22638 [hep-th]] [Search inSPIRE].
[16] K. Falls, [arXiv:2503.05869 [hep-th]] [Search inSPIRE].
[17] G. Bergner, F. Bruckmann, Y. Echigo, Y. Igarashi, J. M. Pawlowski, and S. Schierenberg, Phys. Rev. D **87**, 094516 (2013) [arXiv:1212.0219 [hep-lat]] [Search inSPIRE].

[18] Y. Igarashi, K. Itoh, and T. R. Morris, Prog. Theor. Exp. Phys. **2019**, 103B01 (2019) [arXiv:1904.08231 [hep-th]] [Search inSPIRE].
[19] Y. Igarashi and K. Itoh, Prog. Theor. Exp. Phys. **2021**, 123B06 (2021) [arXiv:2107.14012 [hep-th]] [Search inSPIRE].
[20] Y. Igarashi, K. Itoh, and J. M. Pawlowski, J. Phys. A **49**, 405401 (2016) [arXiv:1604.08327 [hep-th]] [Search inSPIRE].
[21] T. Maskawa and H. Nakajima, Prog. Theor. Phys. **52**, 1326 (1974).
[22] T. Maskawa and H. Nakajima, Prog. Theor. Phys. **54**, 860 (1975).
[23] R. Fukuda and T. Kugo, Nucl. Phys. B **117**, 250 (1976).
[24] V. A. Miransky, Nuov. Cim. A **90**, 149 (1985).
[25] K.-I. Kondo, H. Mino, and K. Yamawaki, Phys. Rev. D **39**, 2430 (1989).
[26] W. A. Bardeen, C. N. Leung, and S. T. Love, Phys. Rev. Lett. **56**, 1230 (1986).
[27] C. N. Leung, S. T. Love, and W. A. Bardeen, Nucl. Phys. B **273**, 649 (1986).
[28] K.-I. Aoki, K.-I. Morikawa, J.-I. Sumi, H. Terao, and M. Tomoyose, Prog. Theor. Phys. **97**, 479 (1997) [arXiv:hep-ph/9612459] [Search inSPIRE].
[29] H. Gies and J. Ziebell, Eur. Phys. J. C **80**, 607 (2020) [arXiv:2005.07586 [hep-th]] [Search inSPIRE].
[30] H. Gies, K. K. K. Tam, and J. Ziebell, Eur. Phys. J. C **83**, 955 (2023) [arXiv:2210.11927 [hep-th]] [Search inSPIRE].
[31] M. Bonini, M. D'Attanasio, and G. Marchesini, Nucl. Phys. B **437**, 163 (1995) [arXiv:hep-th/9410138] [Search inSPIRE].
[32] U. Ellwanger, M. Hirsch, and A. Weber, Z. Phys. C **69**, 687 (1996) [arXiv:hep-th/9506019] [Search inSPIRE].
[33] U. Ellwanger, M. Hirsch, and A. Weber, Eur. Phys. J. C **1**, 563 (1998) [arXiv:hep-ph/9606468] [Search inSPIRE].
[34] B. Bergerhoff and C. Wetterich, Phys. Rev. D **57**, 1591 (1998) [arXiv:hep-ph/9708425] [Search in SPIRE].
[35] M. Mitter, J. M. Pawlowski, and N. Strodthoff, Phys. Rev. D **91**, 054035 (2015) [arXiv:1411.7978 [hep-ph]] [Search inSPIRE].
[36] A. K. Cyrol, L. Fister, M. Mitter, J. M. Pawlowski, and N. Strodthoff, Phys. Rev. D **94**, 054005 (2016) [arXiv:1605.01856 [hep-ph]] [Search inSPIRE].
[37] A. K. Cyrol, M. Mitter, J. M. Pawlowski, and N. Strodthoff, Phys. Rev. D **97**, 054006 (2018) [arXiv:1706.06326 [hep-ph]] [Search inSPIRE].
[38] L. Corell, A. K. Cyrol, M. Mitter, J. M. Pawlowski, and N. Strodthoff, SciPost Phys. **5**, 066 (2018) [arXiv:1803.10092 [hep-ph]] [Search inSPIRE].
[39] W.-j. Fu, C. Huang, J. M. Pawlowski, Y.-y. Tan, and L.-j. Zhou, Phys. Rev. D **112**, 054047 (2025) [arXiv:2502.14388 [hep-ph]] [Search inSPIRE].
[40] C. Wetterich, Phys. Lett. B **301**, 90 (1993) [arXiv:1710.05815 [hep-th]] [Search inSPIRE].
[41] T. R. Morris, Int. J. Mod. Phys. A **9**, 2411 (1994) [arXiv:hep-ph/9308265] [Search inSPIRE].
[42] M. Bonini, M. D'Attanasio, and G. Marchesini, Nucl. Phys. B. **409**, 441 (1993) [arXiv:hep-th/9301114] [Search inSPIRE].
[43] U. Ellwanger, Z. Phys. C **62**, 503 (1994) [arXiv:hep-ph/9308260] [Search inSPIRE].
[44] H. Gies and J. Jaeckel, Phys. Rev. Lett. **93**, 110405 (2004) [arXiv:hep-ph/0405183] [Search inSPIRE].
[45] H. Gies, J. Jaeckel, and C. Wetterich, Phys. Rev. D **69**, 105008 (2004) [arXiv:hep-ph/0312034] [Search inSPIRE].

Funded by SCOAP^3